

NASA TM X-188



1N-08
397278
50p

TECHNICAL MEMORANDUM

X-188

AN EXPERIMENTAL INVESTIGATION TO DETERMINE THE EFFECT OF
SPEED-BRAKE POSITION ON THE LONGITUDINAL STABILITY
AND TRIM OF A SWEEP-WING FIGHTER AIRPLANE

By Robert T. Taylor

Langley Research Center
Langley Field, Va.

Library NASA-HSFS

SEP 28 1959

REVIEW
COPY

CLASSIFIED DOCUMENT - TITLE UNCLASSIFIED

This material contains information affecting the national defense of the United States within the meaning of the espionage laws, Title 18, U.S.C., Secs. 793 and 794, the transmission or revelation of which in any manner to an unauthorized person is prohibited by law.

NATIONAL AERONAUTICS AND SPACE ADMINISTRATION
WASHINGTON

1950

1

1950

[REDACTED]

NATIONAL AERONAUTICS AND SPACE ADMINISTRATION

TECHNICAL MEMORANDUM X-188

AN EXPERIMENTAL INVESTIGATION TO DETERMINE THE EFFECT OF
SPEED-BRAKE POSITION ON THE LONGITUDINAL STABILITY
AND TRIM OF A SWEEP-WING FIGHTER AIRPLANE*

By Robert T. Taylor

ABSTRACT

A 0.10-scale model of a swept-wing fighter airplane was tested in the Langley high-speed 7- by 10-foot tunnel at Mach numbers from 0.60 to 0.92 to determine the effects of adding underfuselage speed brakes. The results of brief spoiler-aileron lateral control tests also are included. The tests show acceptable trim and drag increments when the speed brakes are installed at the 32.71-inch fuselage station.

INDEX HEADINGS

Controls, Spoiler - Complete Wings	1.2.2.4.2
Stability, Longitudinal - Static	1.8.1.1.1
Control, Lateral	1.8.2.2
Airbrakes	1.8.2.4
Control, Hinge Moments	1.8.2.5

*Title, Unclassified.

[REDACTED]



[REDACTED]

NATIONAL AERONAUTICS AND SPACE ADMINISTRATION

TECHNICAL MEMORANDUM X-188

AN EXPERIMENTAL INVESTIGATION TO DETERMINE THE EFFECT OF
SPEED-BRAKE POSITION ON THE LONGITUDINAL STABILITY
AND TRIM OF A SWEEP-WING FIGHTER AIRPLANE*

By Robert T. Taylor

SUMMARY

A 0.10-scale model of a swept-wing fighter airplane was tested in the Langley 7- by 10-foot high-speed tunnel to determine the effect of speed brakes under and at the sides of the fuselage on the longitudinal stability and trim over the airplane Mach number range. The results of brief lateral control tests concerning (1) the effect of a plain spoiler mounted ahead of the aileron and (2) the effect of blunting the aileron trailing edge are included also.

An adequate drag increment with an acceptable pitch increment was obtained when both the side and underfuselage speed brakes were extended 50° and with the underfuselage brakes mounted in their most forward position.

The addition of spoilers ahead of the aileron, when located at the inboard station, reduced the aileron hinge-moment characteristics. Blunting the aileron trailing edge changed the effectiveness only slightly and reduced the aileron hinge moments by approximately 40 percent.

INTRODUCTION

Interest in a particular mission for a swept-wing fighter airplane dictated the use of additional speed brakes on the underside of the fuselage. Inasmuch as negative trim angle-of-attack changes accompanying speed-brake deflection are objectionable, it was considered desirable to determine experimentally the speed-brake hinge-line location which would give zero or slightly positive trim angle-of-attack changes under full brake application. An investigation was therefore made in the Langley

*Title, Unclassified.


high-speed 7- by 10-foot tunnel to assess the effect of varying the under-fuselage speed-brake hinge-line location. Brief lateral control tests were also made to determine the effects of installing a spoiler ahead of the aileron hinge line and blunting the aileron trailing edge. The results of these wind-tunnel tests are presented herein.

SYMBOLS

The direction of positive forces, moments, and angles is shown in figure 1.

A	area moment of aileron normal to hinge line, cu ft
b	wing span, ft
c	wing chord, ft
\bar{c}	wing mean aerodynamic chord, ft
C_a	aileron chord, ft
C_D	drag coefficient, $\frac{F_D}{qS}$
C_h	aileron hinge-moment coefficient, $\frac{M_H}{qA}$
$C_{h\alpha}$	rate of change of hinge-moment coefficient with angle of attack, taken at $\alpha = 0^\circ$, $\frac{\partial C_h}{\partial \alpha}$
$C_{h\delta_a}$	rate of change of hinge-moment coefficient with aileron deflection, taken from $\delta_a = 0^\circ$ to -5° , $\frac{\partial C_h}{\partial \delta_a}$
C_L	lift coefficient, $\frac{F_L}{qS}$
C_l	rolling-moment coefficient, $\frac{M_x}{qSb}$
$C_{l\delta_a}$	rate of change of rolling-moment coefficient with aileron deflection, taken from $\delta_a = 0^\circ$ to -5° , $\frac{\partial C_l}{\partial \delta_a}$
C_m	pitching-moment coefficient (moments taken about $\frac{\bar{c}}{4}$), $\frac{M_y}{qS\bar{c}}$

$\left(\frac{\Delta C_m}{\delta_{50}}\right)_{C_L=0.2}$	increment in pitching moment due to deflecting underfuselage and side speed brakes 50° at a lift coefficient of $C_L = 0.2$
C_n	yawing-moment coefficient, $\frac{M_z}{qSb}$
C_Y	side-force coefficient, $\frac{F_Y}{qS}$
F_D	drag, lb
F_L	lift, lb
F_Y	side force, lb
M	Mach number
M_H	aileron hinge moment, ft-lb
M_X	rolling moment, ft-lb
M_{Yw}	pitching moment, ft-lb
M_Z	yawing moment, ft-lb
q	free-stream dynamic pressure, $\frac{1}{2} \rho V^2$, lb/sq ft
R	Reynolds number
S	wing area, sq ft
V	free-stream velocity, ft/sec
α	angle of attack, deg
δ_a	aileron deflection, deg
δ_G	speed-brake fuselage gap, in.
δ_B	side speed-brake deflection, deg
δ_u	underfuselage speed-brake deflection, deg
ρ	free-stream density, slugs/cu ft


APPARATUS AND TESTS

A 0.10-scale manufacturer's model of a current jet fighter airplane was used in the investigation. The model consisted of aluminum wings and tail surfaces mounted on a steel fuselage core. The fuselage core was covered with wood, which formed the exterior fuselage shape.

Photographs of the model mounted for testing in the Langley high-speed 7- by 10-foot tunnel are presented as figure 2. Figure 3 shows pertinent model geometry with sketches of the speed brakes and controls tested.

As is shown in figure 3(a), the model was tested with the underfuselage brakes at four longitudinal stations at several brake deflections and brake-fuselage gaps. Details of the underfuselage brakes are shown in figure 3(b). Lateral control tests were also made with the original conventional aileron and with a blunt-trailing-edge aileron suggested by the manufacturer, with and without 0.058 spoilers mounted in the various positions shown in figure 3(a). Typical aileron cross sections are shown in figure 3(c).


The model was installed on a six-component strain-gage balance, the output of which was fed to recording potentiometers. Aileron hinge-moment data also were recorded with this equipment.

Tests were made in the Langley high-speed 7- by 10-foot tunnel at Mach numbers from 0.60 to 0.92. The variation in test Reynolds number as a function of Mach number is presented in figure 4.

CORRECTIONS

The data presented have been corrected for the effects of tunnel blockage at zero lift by the method of reference 1. The effects of stream constraint have been accounted for by the method of reference 2. The effects of base-pressure drag have been eliminated; that is, all the drag data have been corrected to conditions of tunnel free-stream static pressure at the model base. Corrections to the angle of attack due to sting and balance deflection under load also have been applied.

The tests made with the spoiler mounted ahead of the aileron do not include the rolling moment, yawing moment, or side force due to the spoiler since an identical spoiler was used on the opposite wing at the inboard station. (See fig. 2(a).)



PRESENTATION OF RESULTS

The results obtained are outlined in the following table:

	Figure
Effect of underfuselage speed-brake deflection	5
Effect of fuselage side brakes	6
Effect of underfuselage speed-brake gap	7
Effect of underfuselage speed-brake longitudinal position . . .	8
Effect of fuselage side brakes on effectiveness of the underfuselage brakes	9
Effectiveness of conventional aileron	10
Aileron effectiveness in presence of inboard spoiler	11
Aileron effectiveness in presence of outboard spoiler	12
Comparison of conventional and blunt trailing-edge aileron effectiveness	13
Summary of pitch increments due to deflecting all speed brakes 50°	14
Summary of aileron effectiveness including the effect of blunting the aileron trailing edge and of installing spoilers ahead of the aileron at two spanwise locations . . .	15

DISCUSSION

The data are presented with a minimum of discussion; however, it should be pointed out that an increment in drag ΔC_D of about 0.02 was obtained, due to deflecting the underfuselage brakes 50° throughout the Mach number range investigated (figs. 5 to 9). The pitching-moment increments due to deflecting side and underfuselage speed brakes 50° are summarized in figure 14. With the underfuselage brakes located at fuselage station 32.71, the most forward location, an acceptable (slightly positive) trim change is present.

The results of the lateral control tests are summarized in figure 15. Addition of the blunt trailing edge to the aileron decreases the aileron effectiveness slightly and decreases the hinge-moment-curve slope approximately 40 percent. The addition of a spoiler ahead of the aileron at the inboard station decreased somewhat the rolling moment due to the aileron and tends to improve the aileron hinge-moment characteristics at the deflections tested. The spoiler installation at the outboard station also decreases the rolling moment due to aileron but has a much less favorable effect on the aileron hinge moment. No dynamic data were taken with spoiler or speed brake extended.

CONCLUDING REMARKS

Results of an experimental wind-tunnel investigation to determine the optimum location for underfuselage speed brakes on a current jet-fighter model have been presented. The most forward location tested provided the least objectionable trim change and still yielded essentially the same increment in drag coefficient.

Langley Research Center,
National Aeronautics and Space Administration,
Langley Field, Va., August 26, 1959.

REFERENCES

1. Herriot, John G.: Blockage Corrections for Three-Dimensional-Flow Closed-Throat Wind Tunnels, With Consideration of the Effect of Compressibility. NACA Rep. 995, 1950. (Supersedes NACA RM A7B28.)
2. Gillis, Clarence L., Polhamus, Edward C., and Gray, Joseph L., Jr.: Charts for Determining Jet-Boundary Corrections for Complete Models in 7- by 10-Foot Closed Rectangular Wind Tunnels. NACA WR L-123, 1945. (Formerly NACA ARR L5G31.)

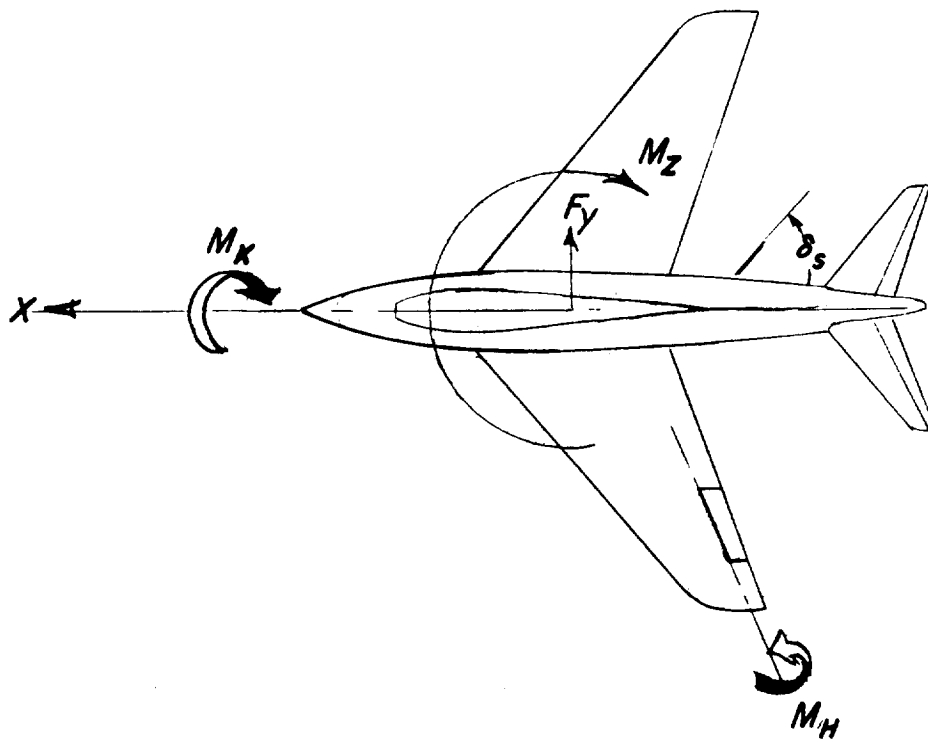
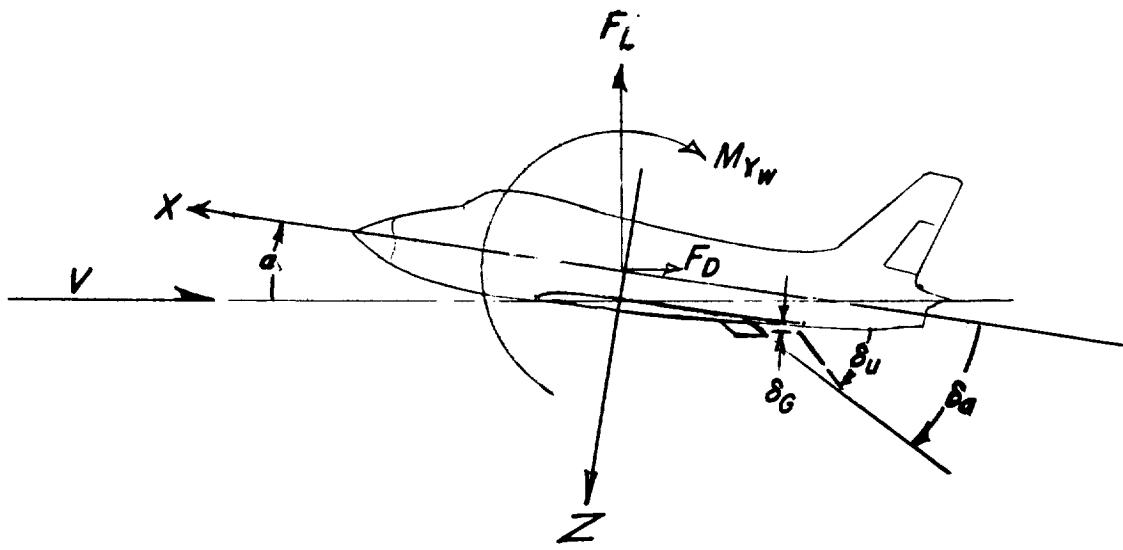
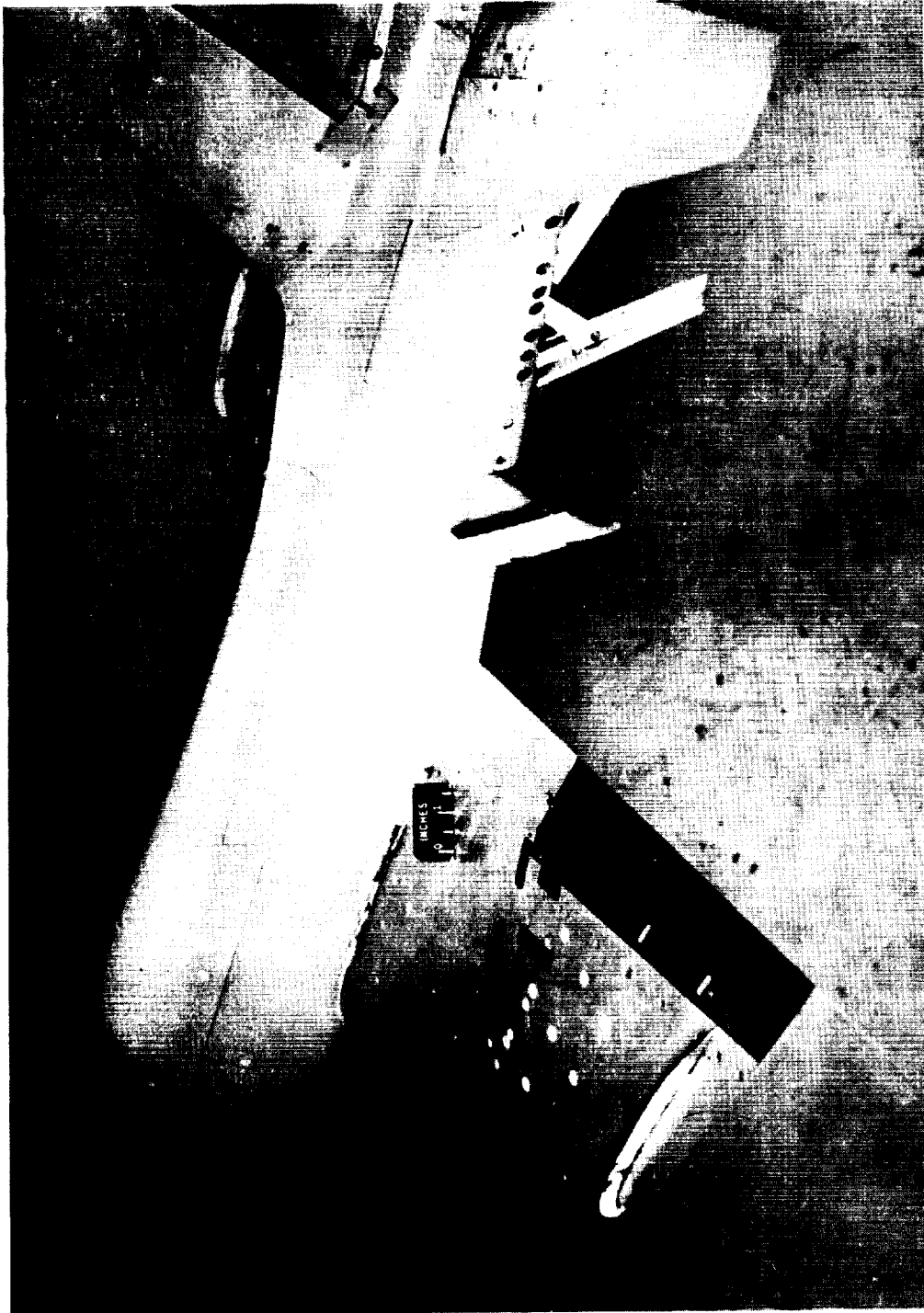


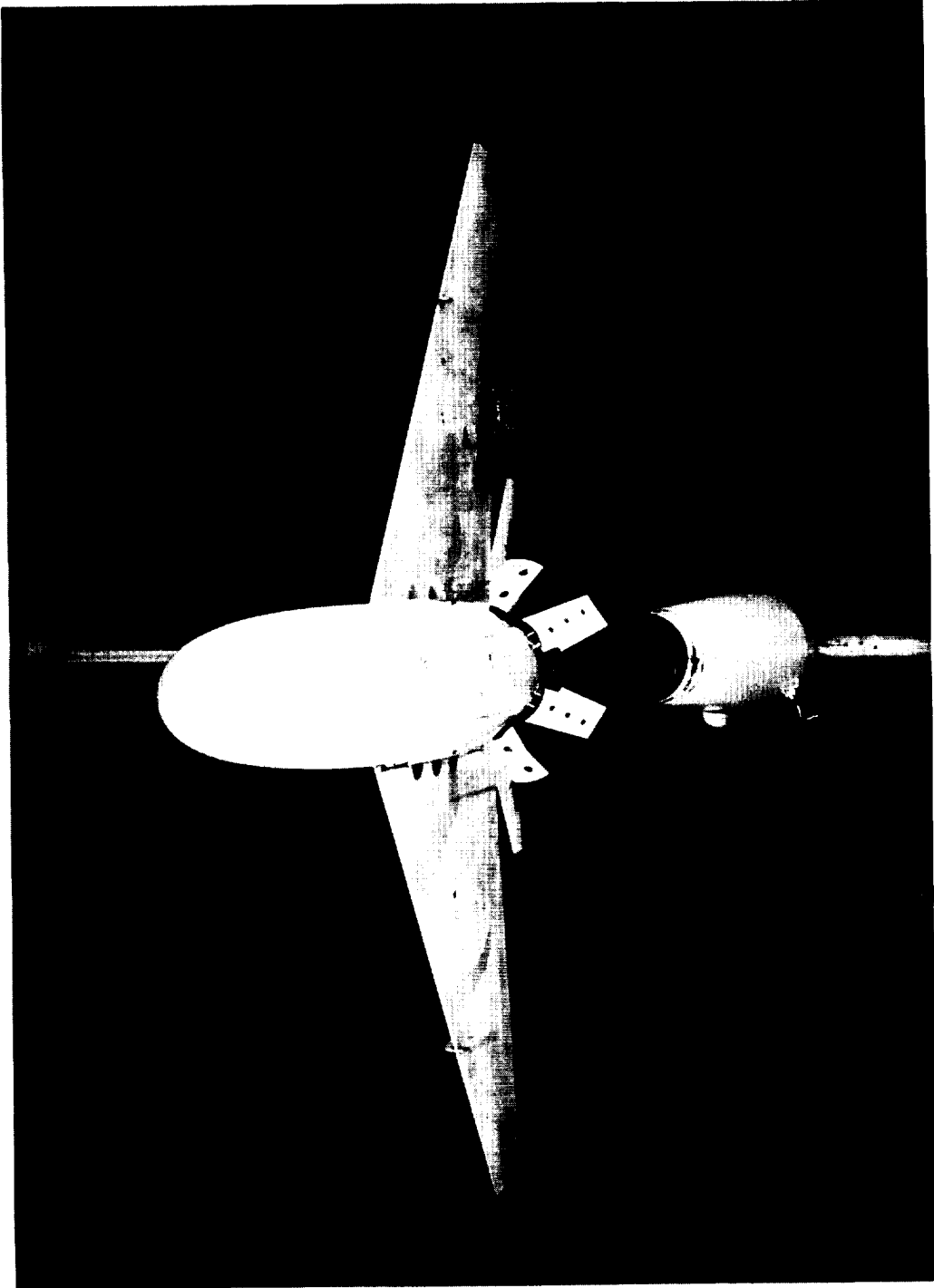
Figure 1.- Sketch showing direction of positive forces, moments, and angles.



(a) Three-quarter rear view. L-94090
Figure 2.- Views of model installed in Langley 7- by 10-foot high-speed tunnel.

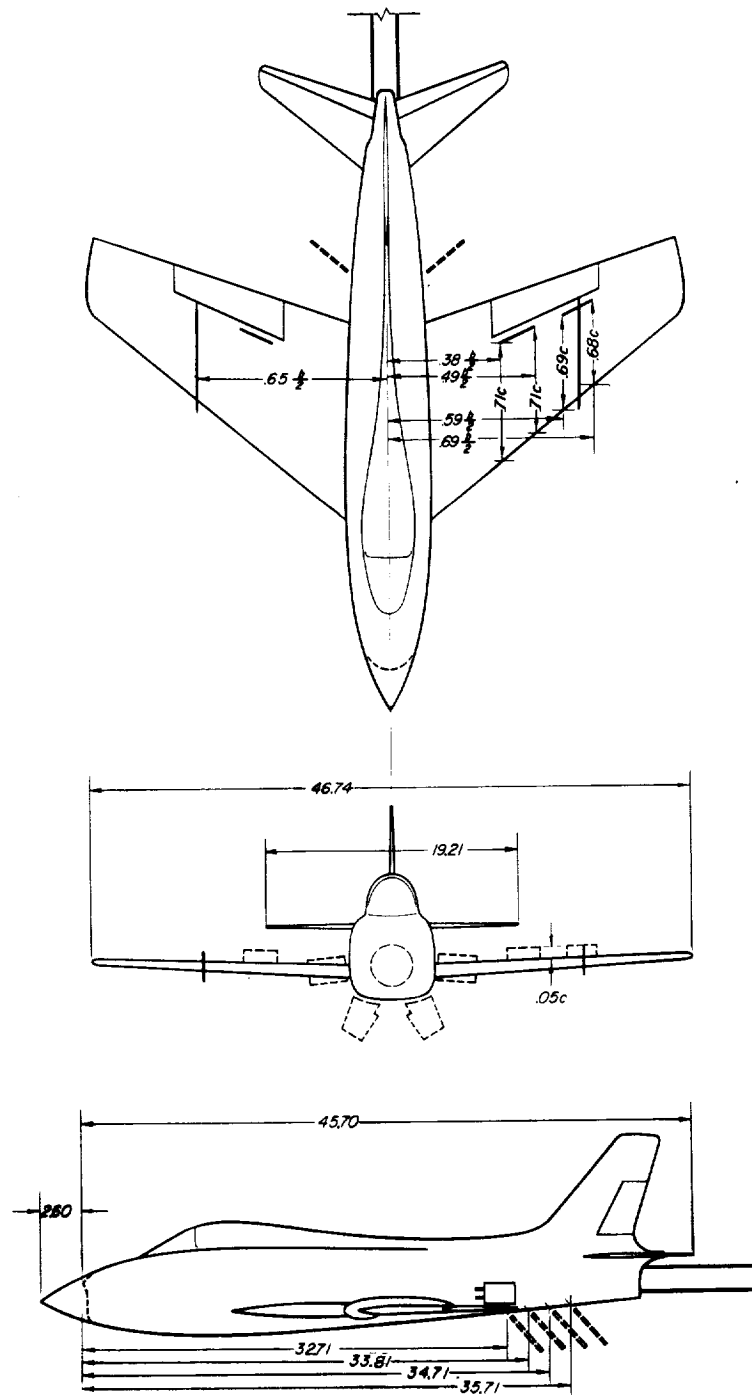
CONFIDENTIAL

CONFIDENTIAL



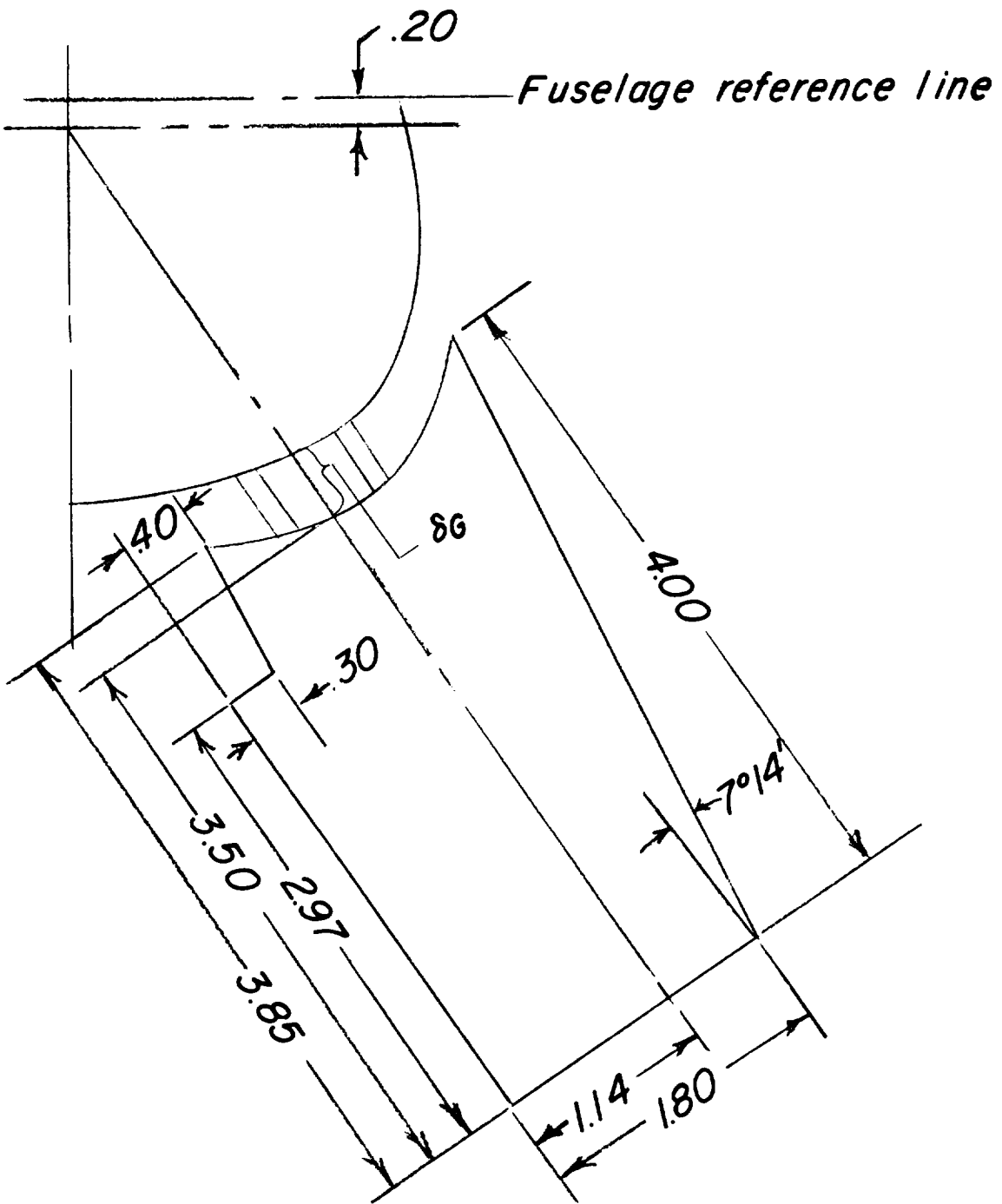
(b) Front view. L-94091

Figure 2.- Concluded.



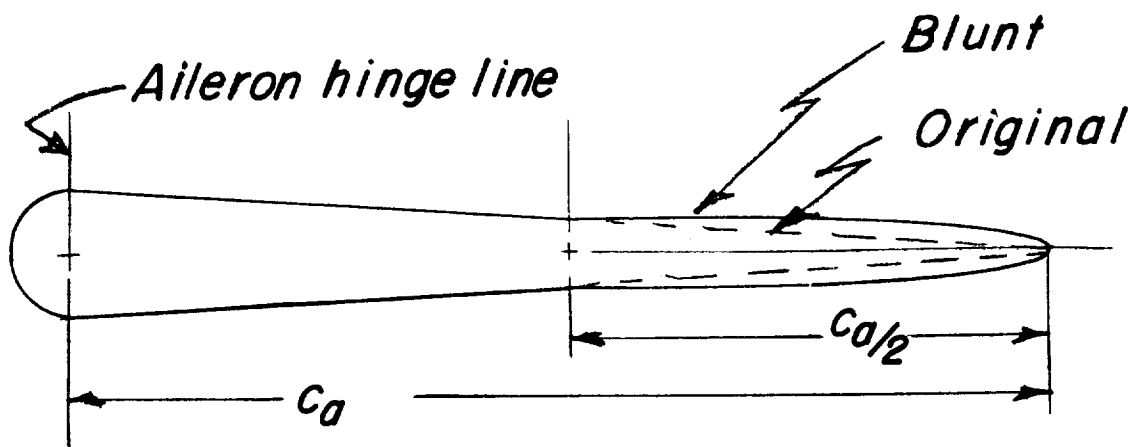
(a) General arrangement.

Figure 3.- Model details. All dimensions are in inches.



(b) Sketch of underfuselage speed brake.

Figure 3.- Continued.



(c) Typical aileron cross sections tested.

Figure 3.- Concluded.

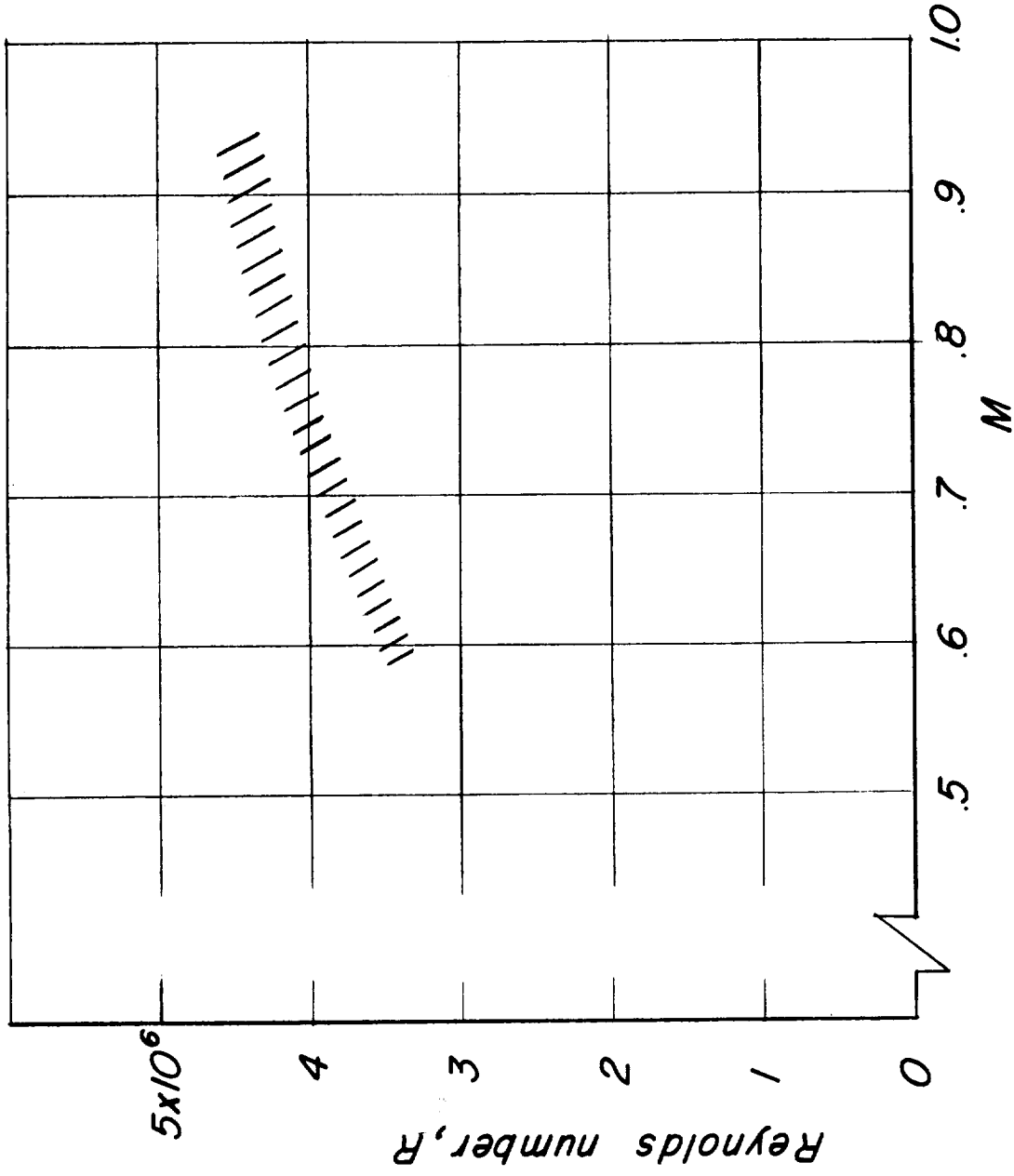
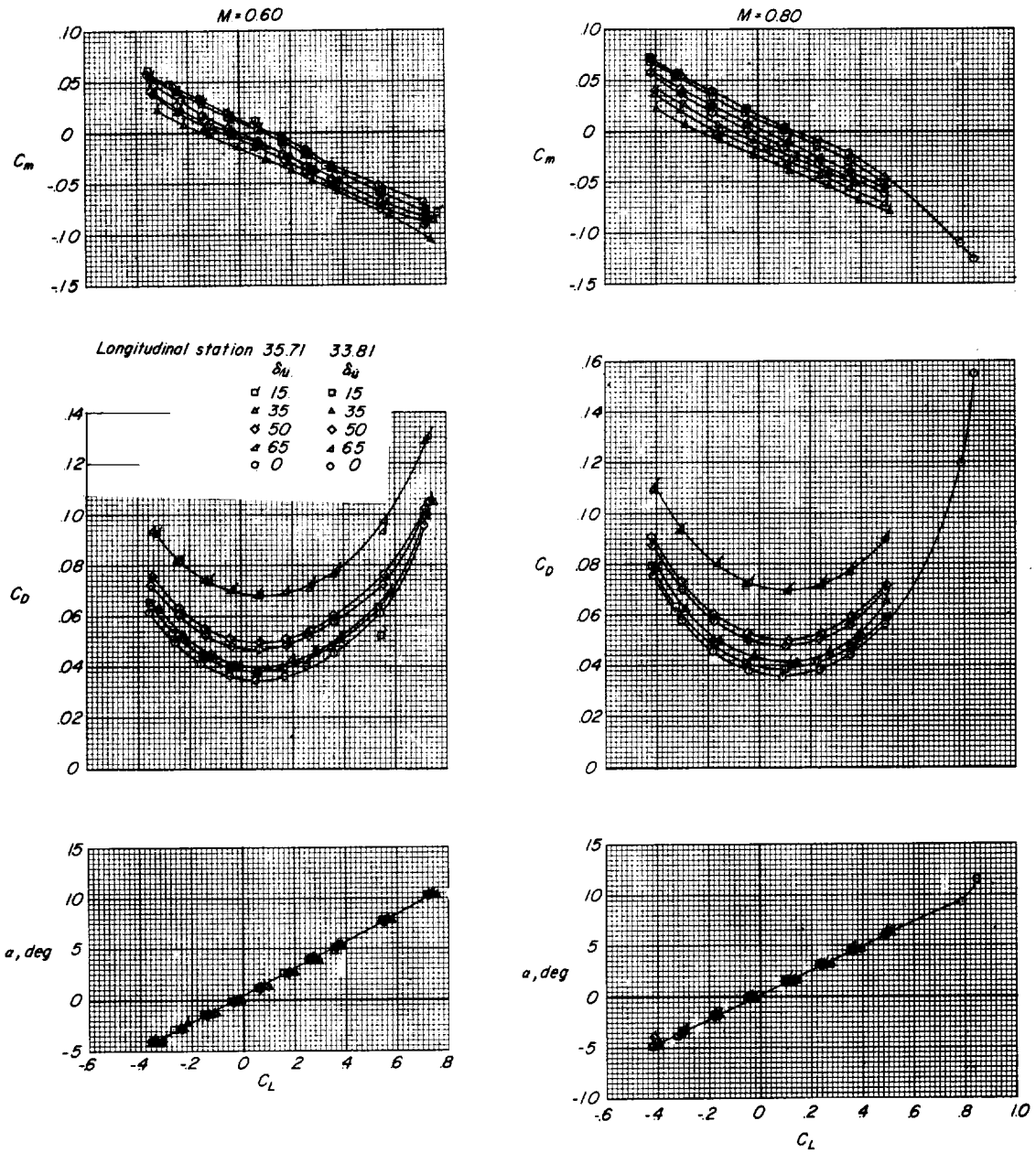
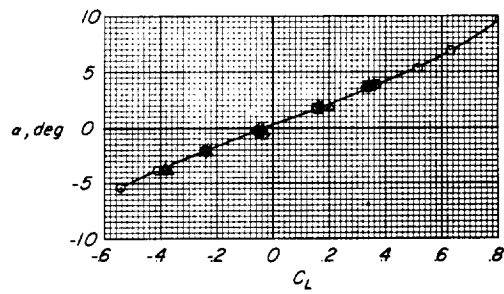
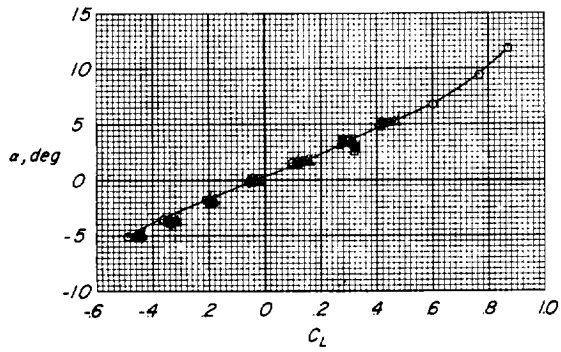
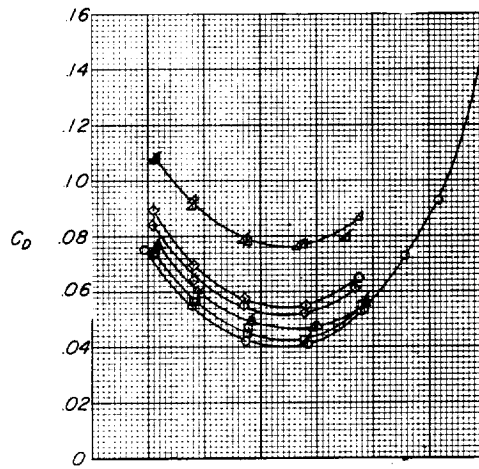
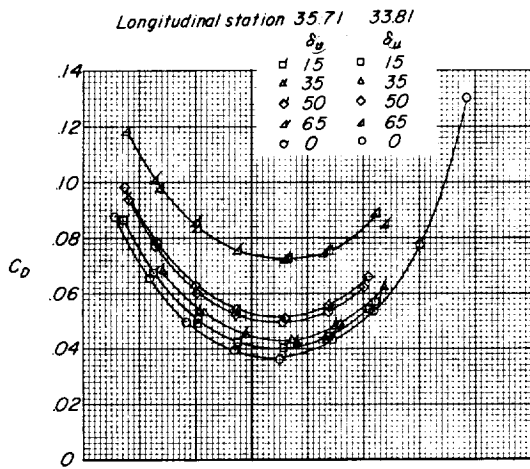
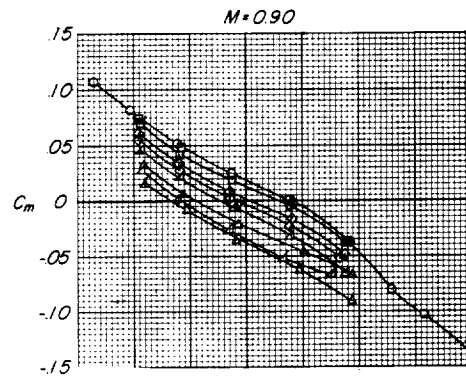
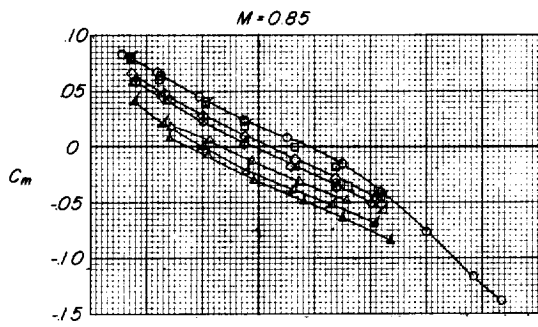


Figure 4.- Approximate variation of Reynolds number with Mach number over range of tests.



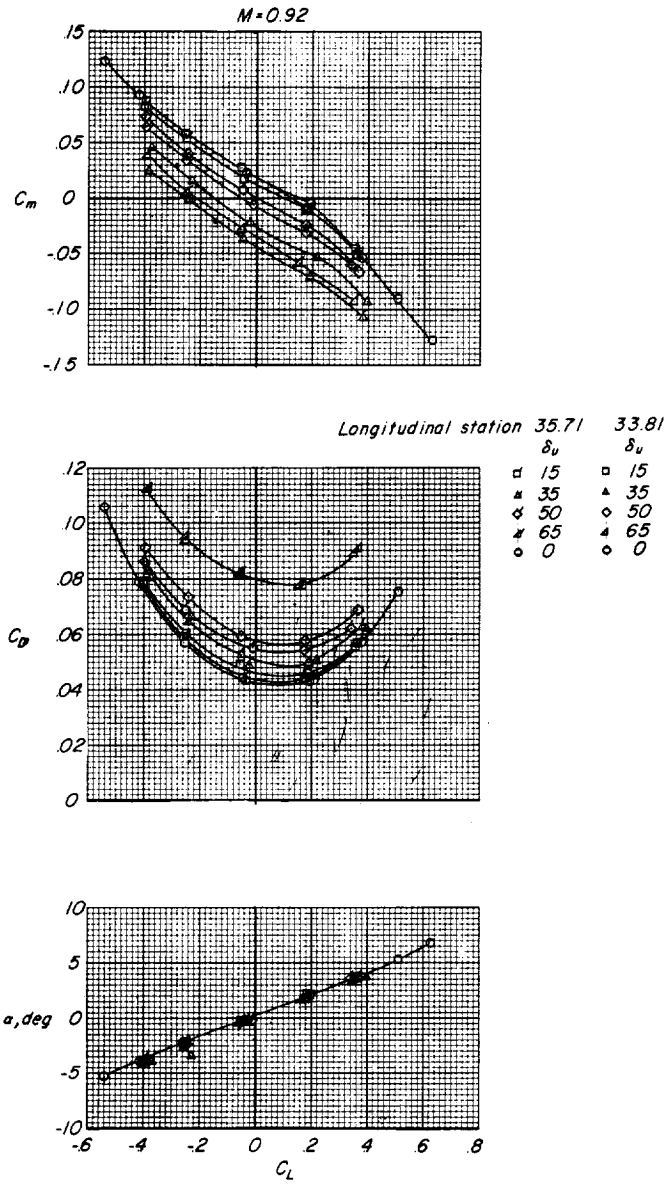
(a) $M = 0.60$ and 0.80 .

Figure 5.- Effect of underfuselage speed-brake deflection on the longitudinal aerodynamic characteristics at two longitudinal underfuselage speed-brake positions. $\delta_s = 50^\circ$; $\delta_G = 0.4$ inch.



(b) $M = 0.85$ and $M = 0.90$.

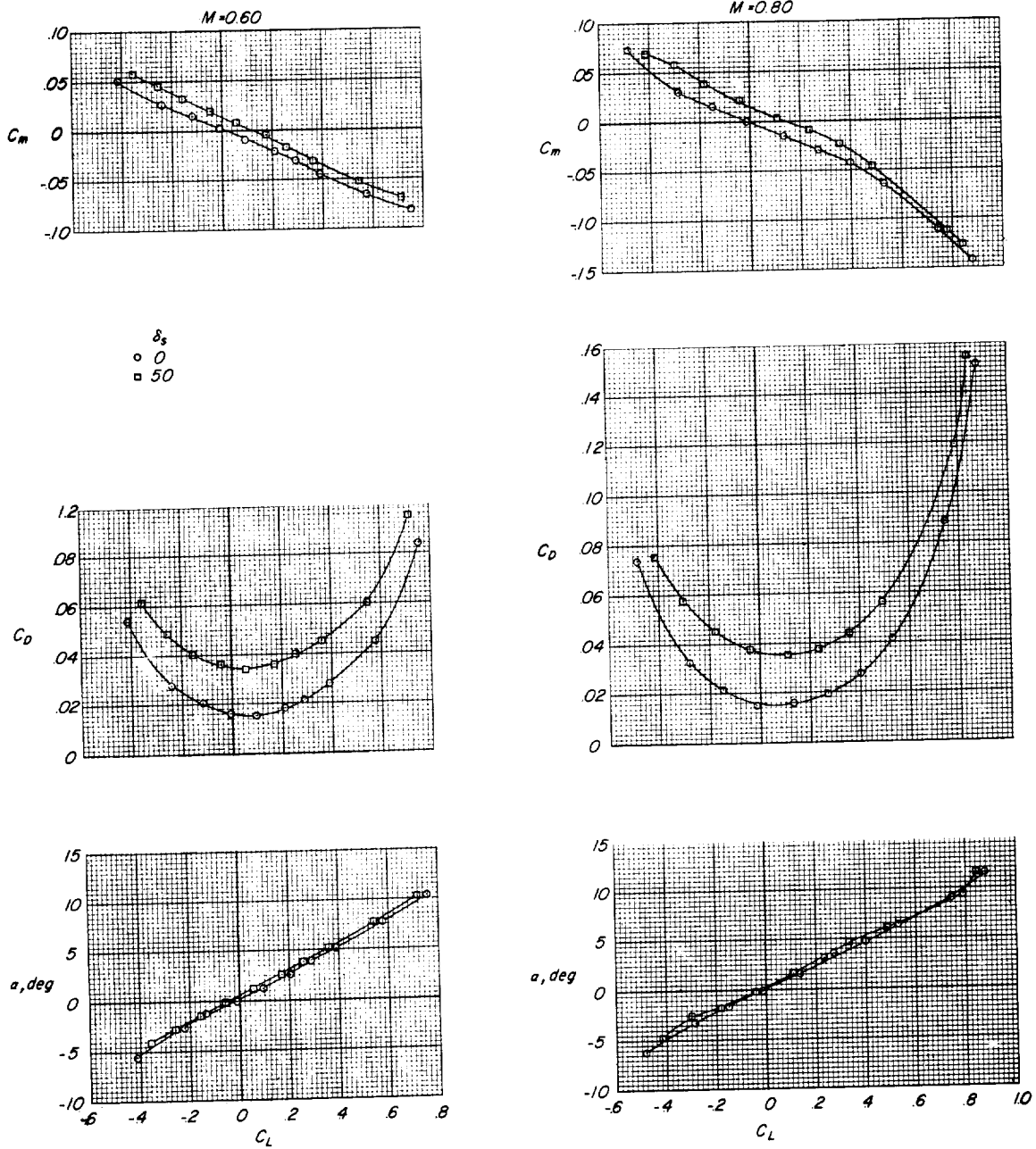
Figure 5.- Continued.



(c) $M = 0.92$.

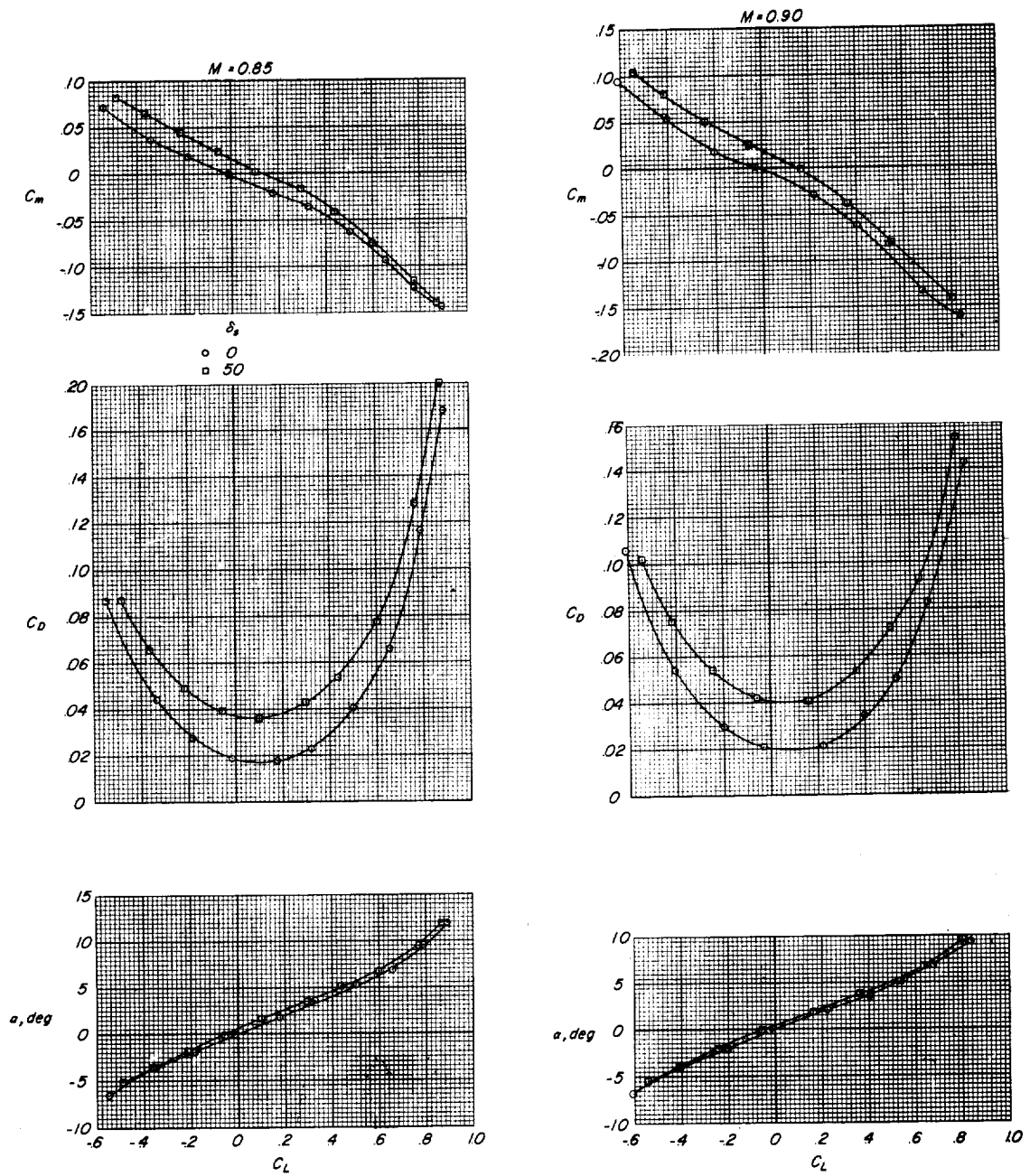
Figure 5.- Concluded.





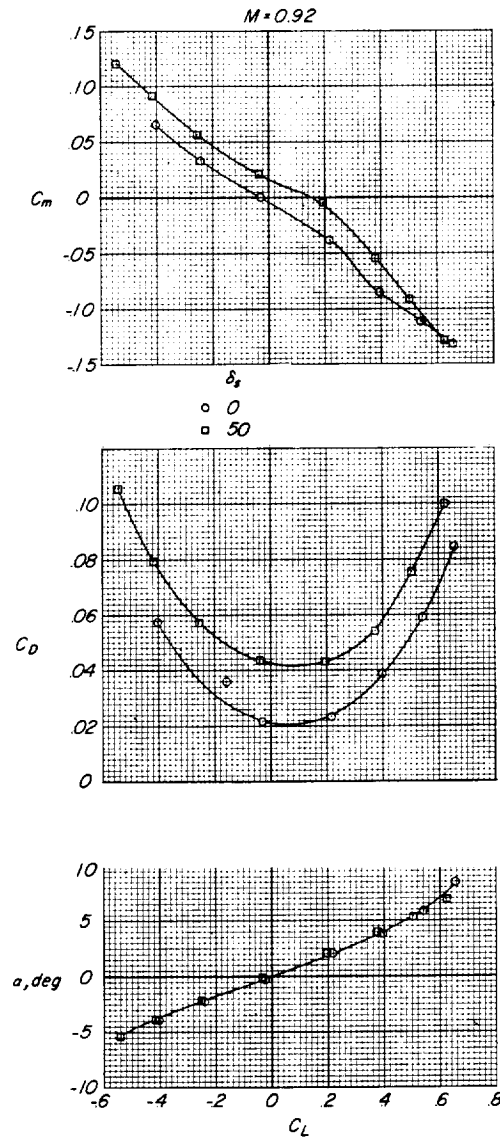
(a) $M = 0.60$ and 0.80 .

Figure 6.- The effect of fuselage side brake on longitudinal aerodynamic characteristics of model. $\delta_u = 0^\circ$.



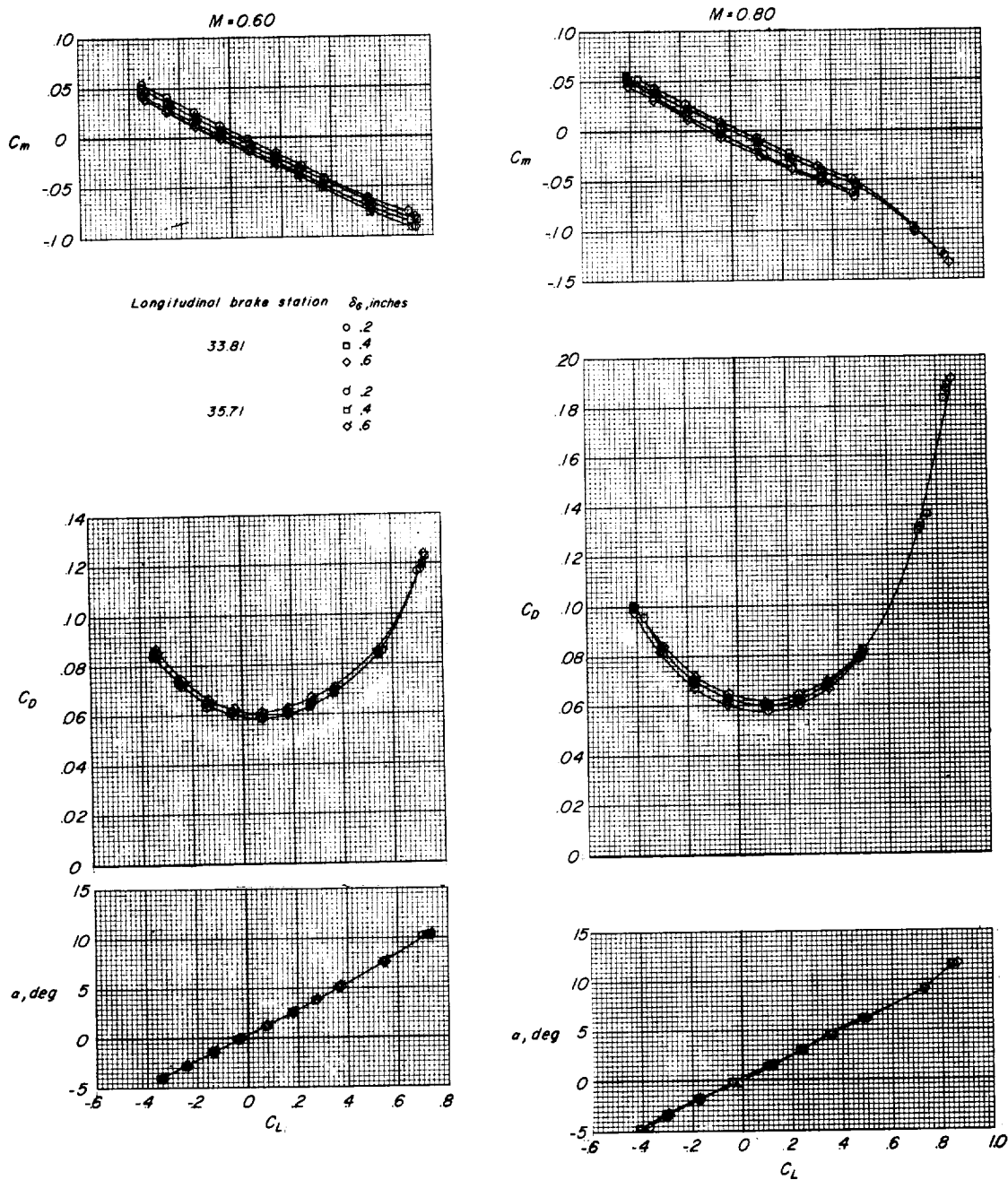
(b) $M = 0.85$ and 0.90 .

Figure 6.- Continued.



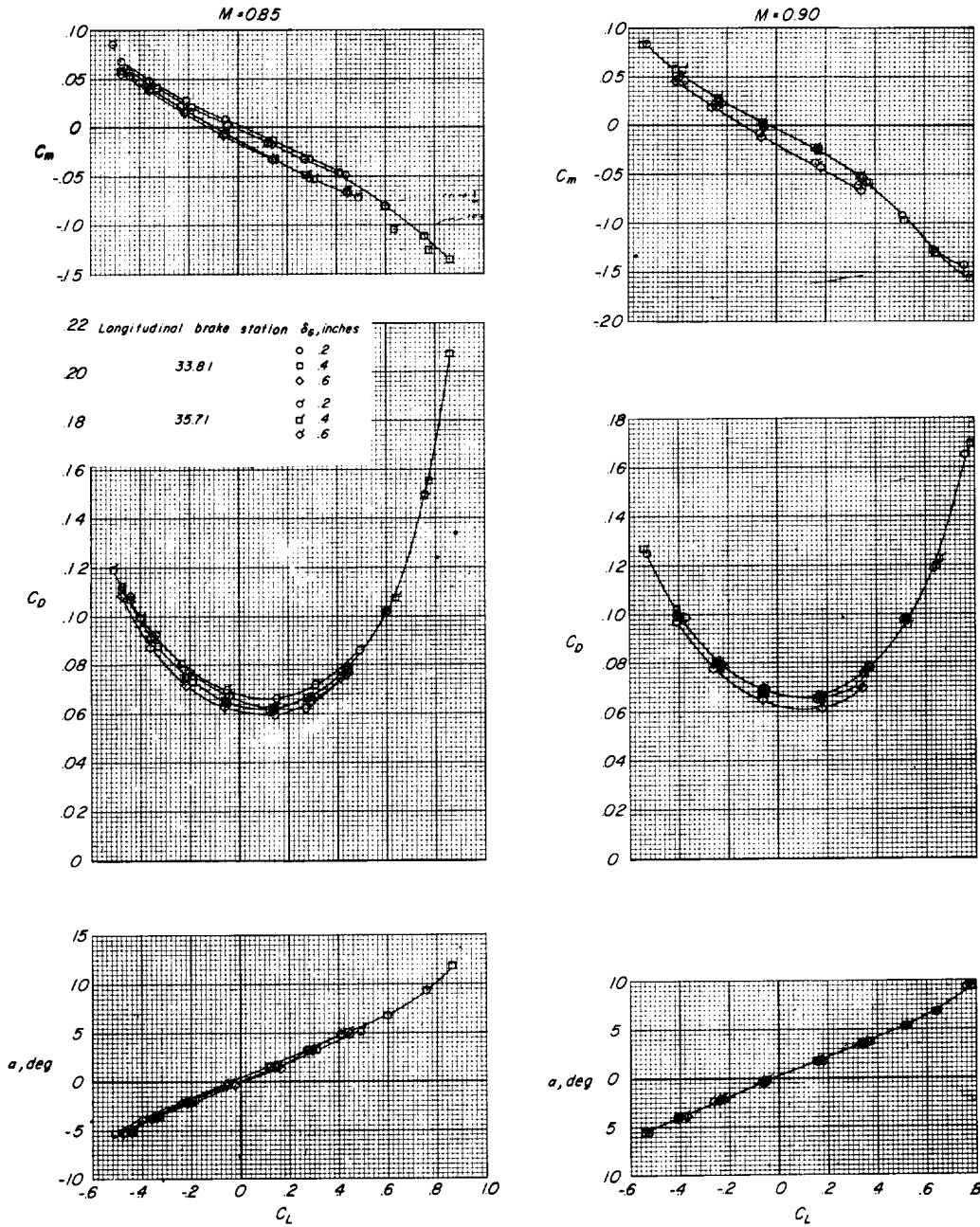
(c) $M = 0.92$.

Figure 6.- Concluded.



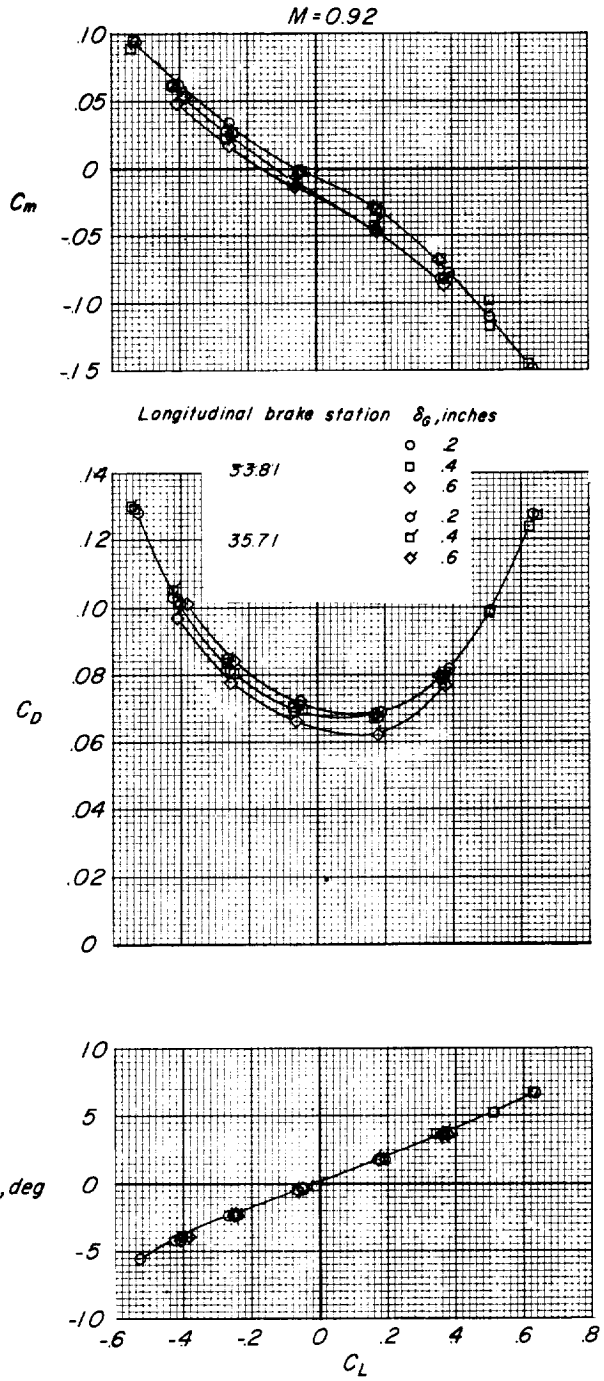
(a) $M = 0.60$ and 0.80 .

Figure 7.- The effect of underfuselage speed-brake gap on longitudinal aerodynamic characteristics at constant speed-brake deflection and at two longitudinal speed-brake positions. $\delta_s = 50^\circ$; $\delta_u = 50^\circ$.



(b) $M = 0.85$ and 0.90 .

Figure 7.- Continued.



(c) $M = 0.92$.

Figure 7.- Concluded.



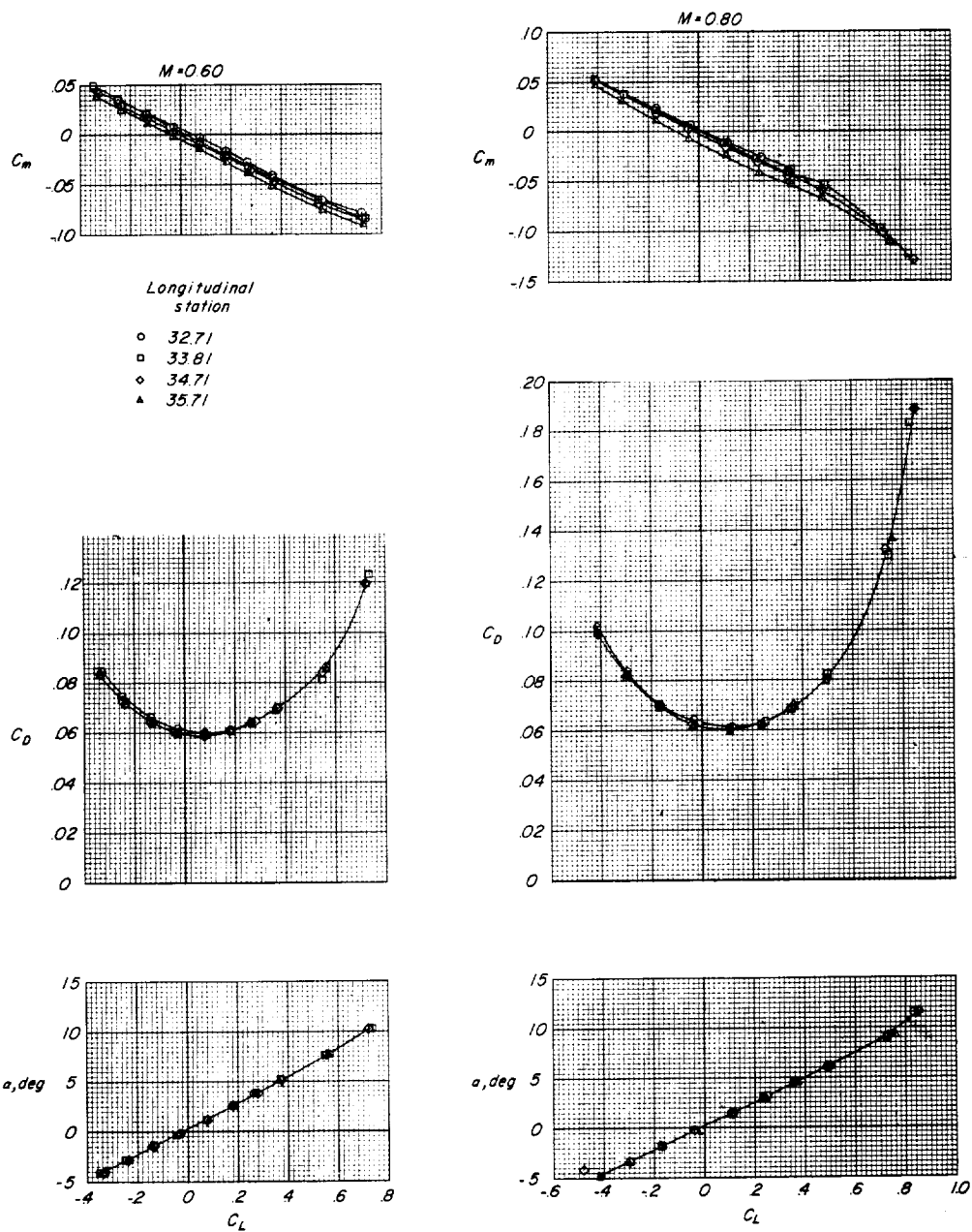
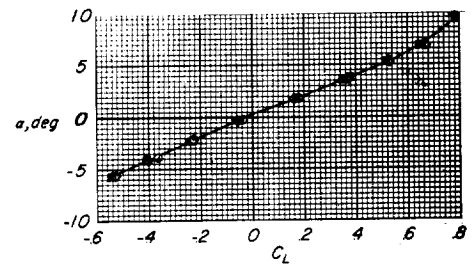
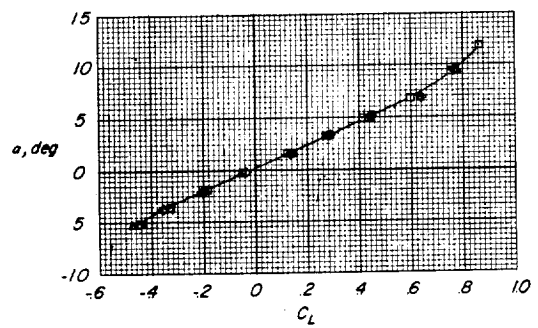
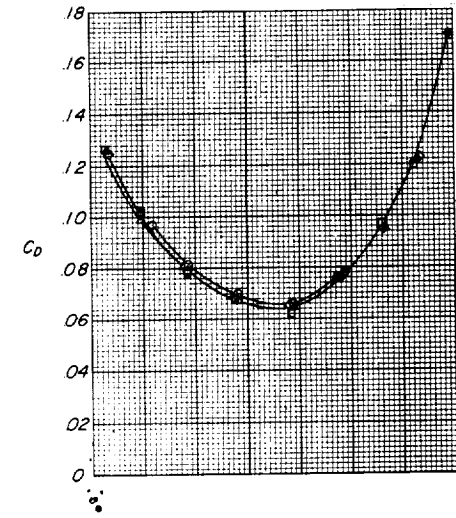
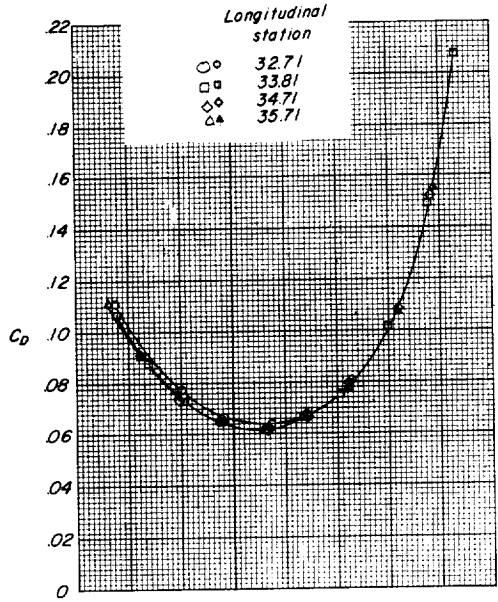
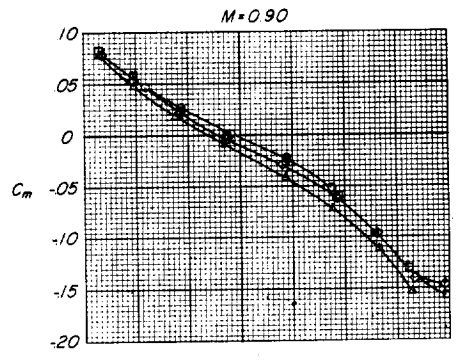
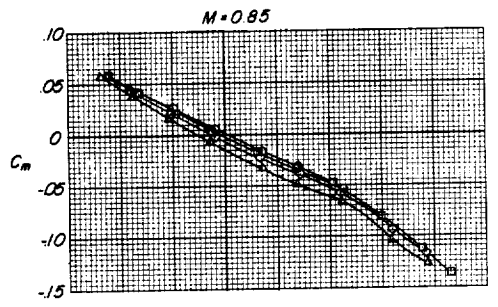
(a) $M = 0.60$ and $M = 0.80$.

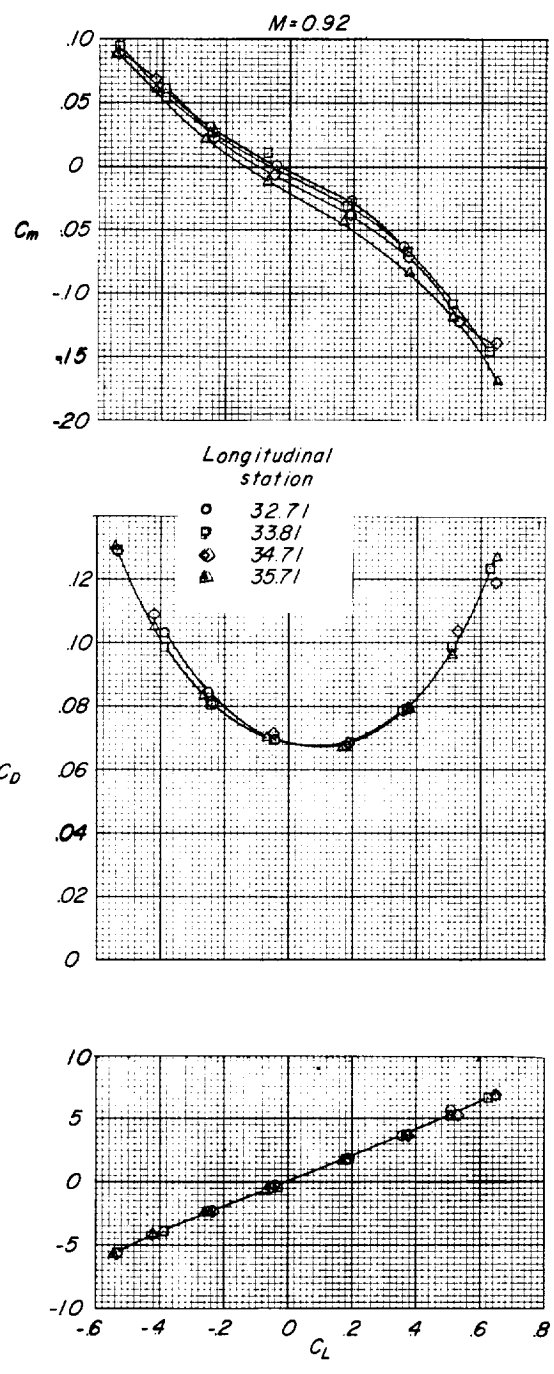
Figure 8.- The effect of underfuselage speed-brake longitudinal position on the longitudinal aerodynamic characteristics at a constant brake deflection and brake gap. $\delta_S = \delta_U = 50^\circ$; $\delta_G = 0.4$ inch.



(b) $M = 0.85$ and $M = 0.90$.

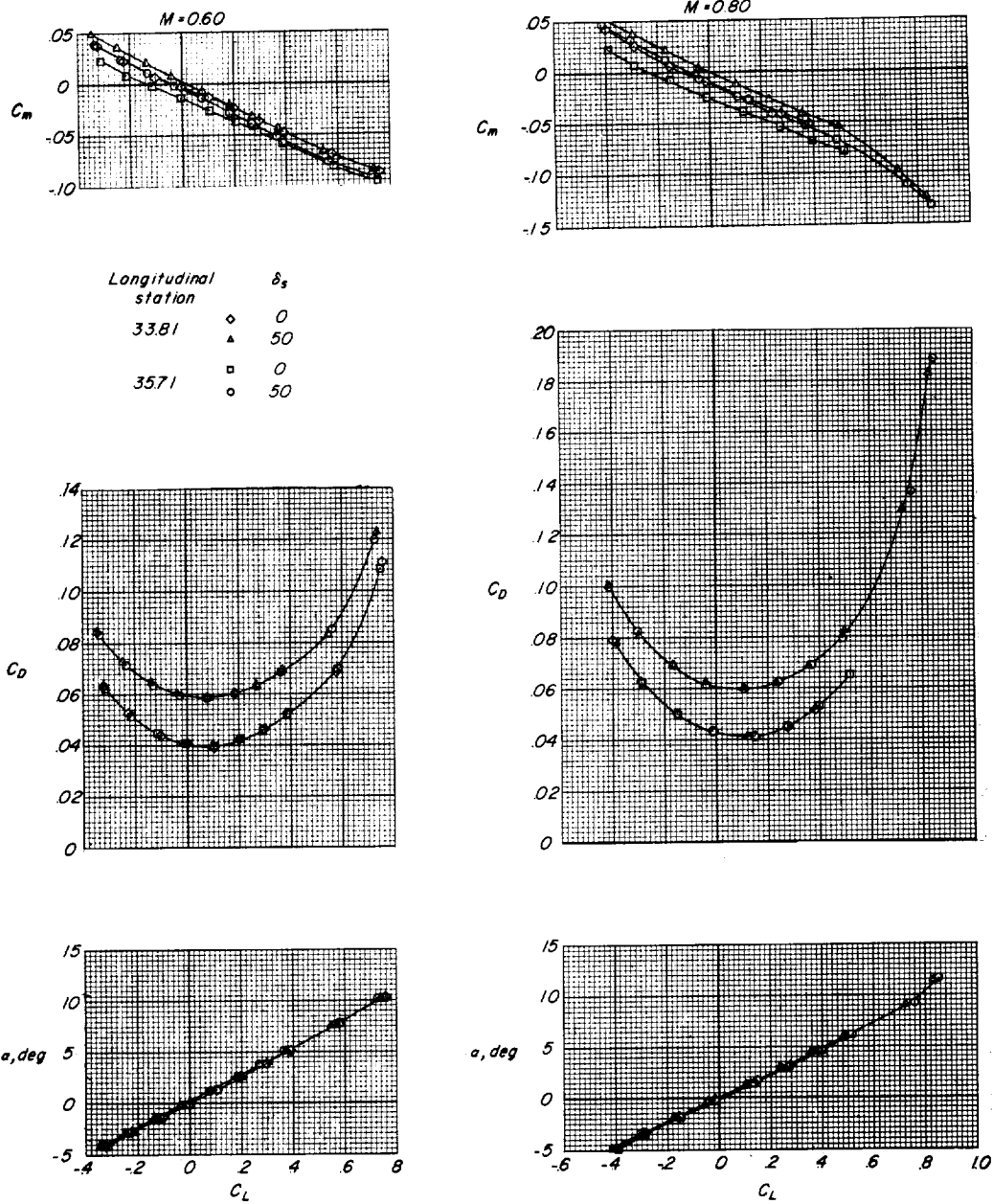
Figure 8.- Continued.





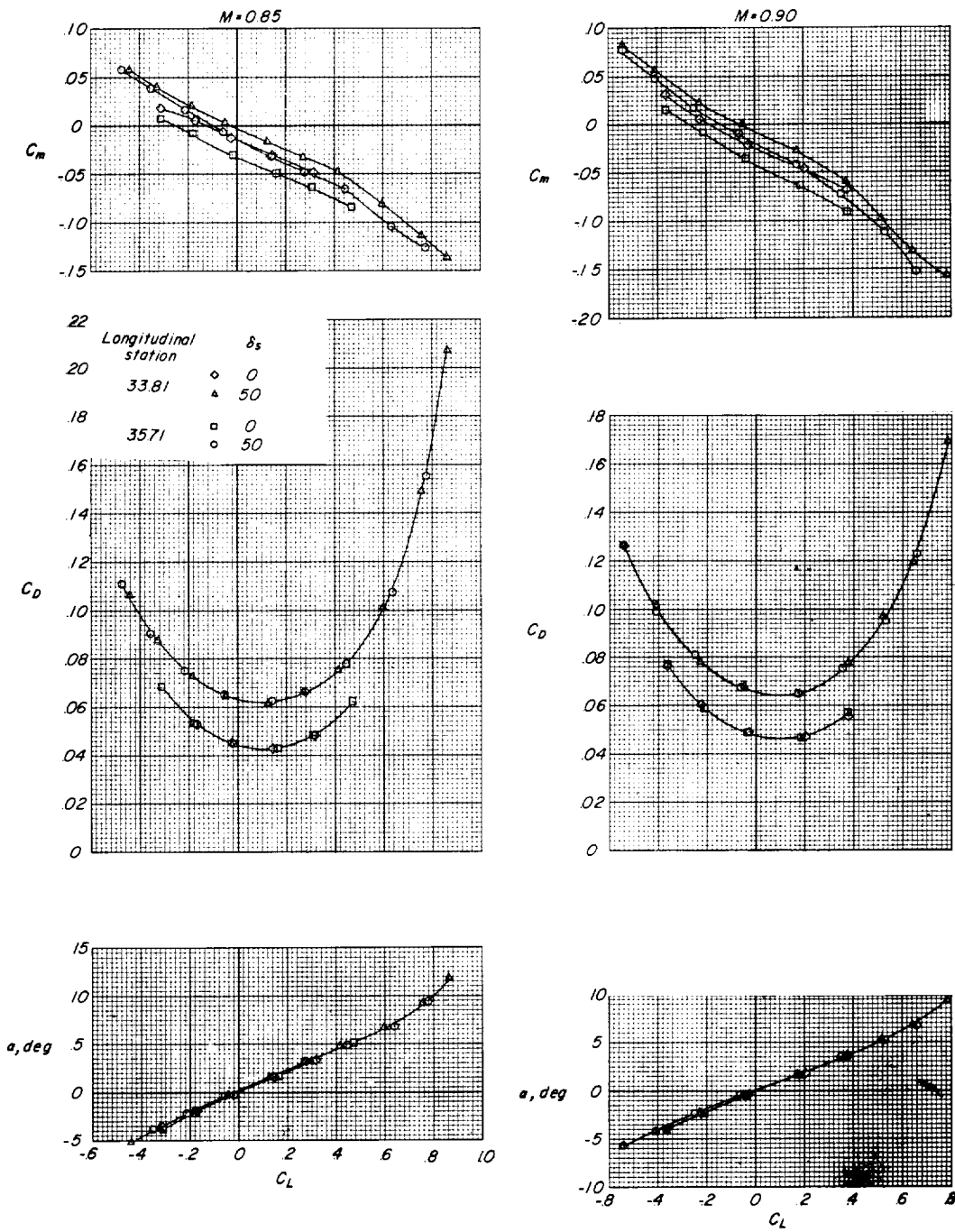
(c) $M = 0.92$.

Figure 8.- Concluded.



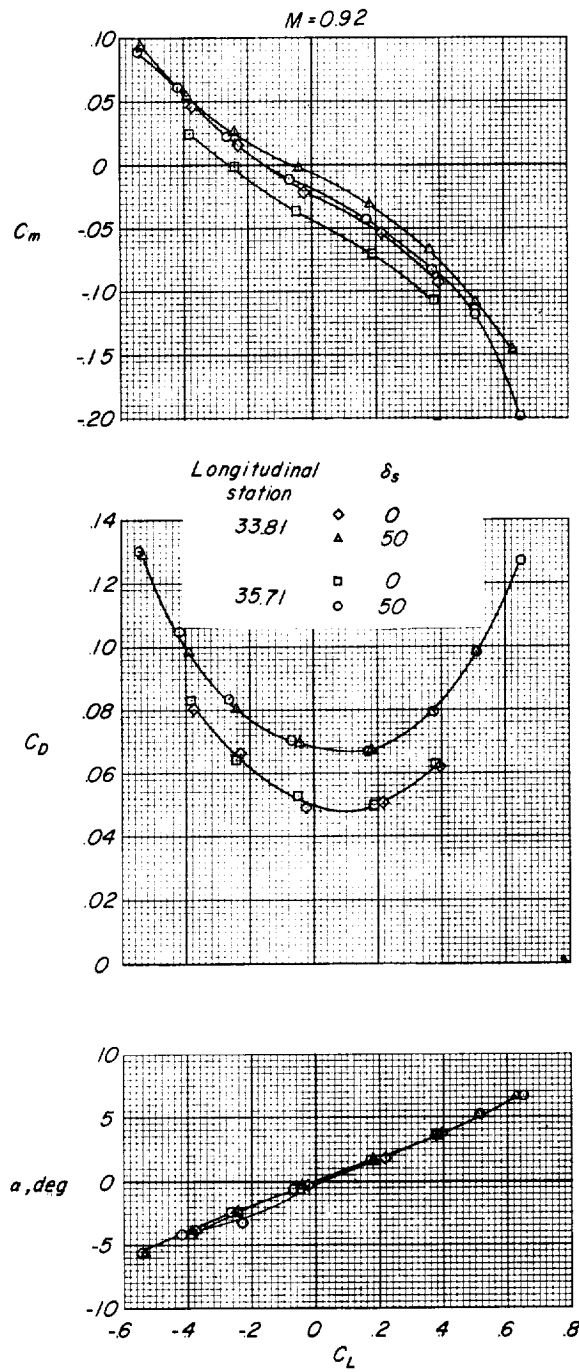
(a) $M = 0.60$ and $M = 0.80$.

Figure 9.- The effect of fuselage side brakes on the longitudinal aerodynamic effectiveness of the underfuselage speed brakes at a constant brake deflection and gap. $\delta_s = \delta_u = 50^\circ$; $\delta_G = 0.4$ inch.



(b) $M = 0.85$ and $M = 0.90$.

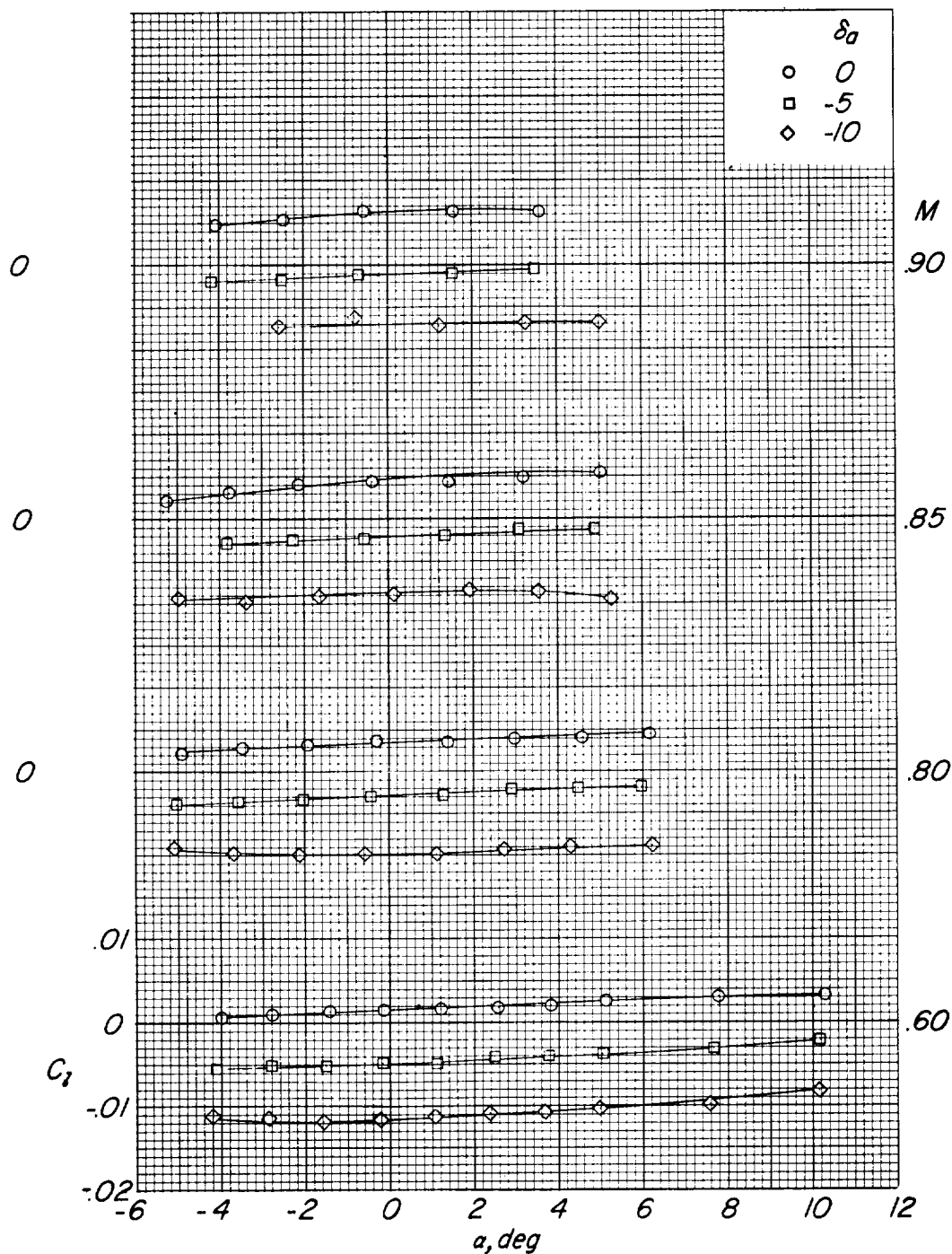
Figure 9.- Continued.



(c) $M = 0.92$.

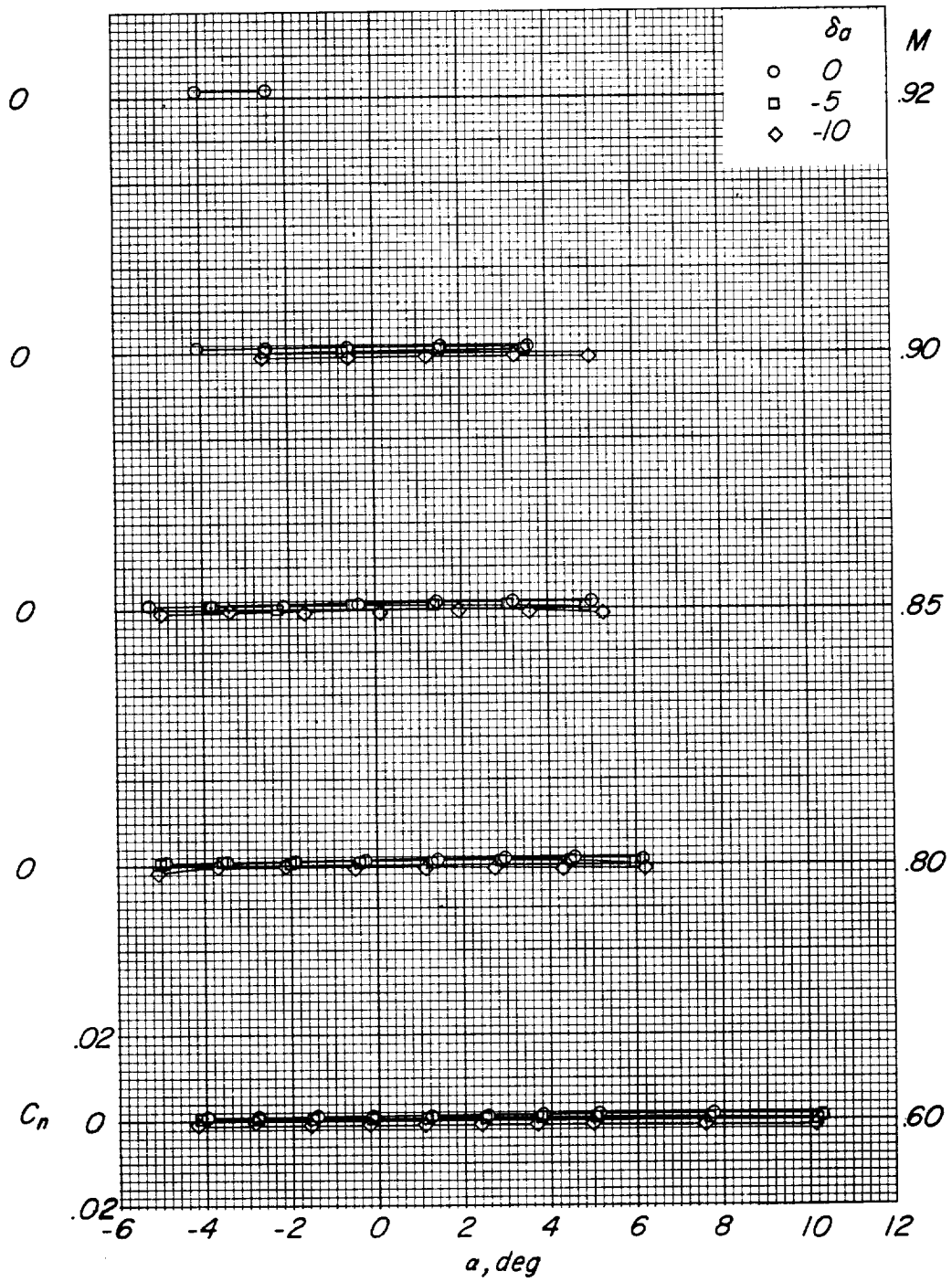
Figure 9.- Concluded.

~~CONFIDENTIAL~~



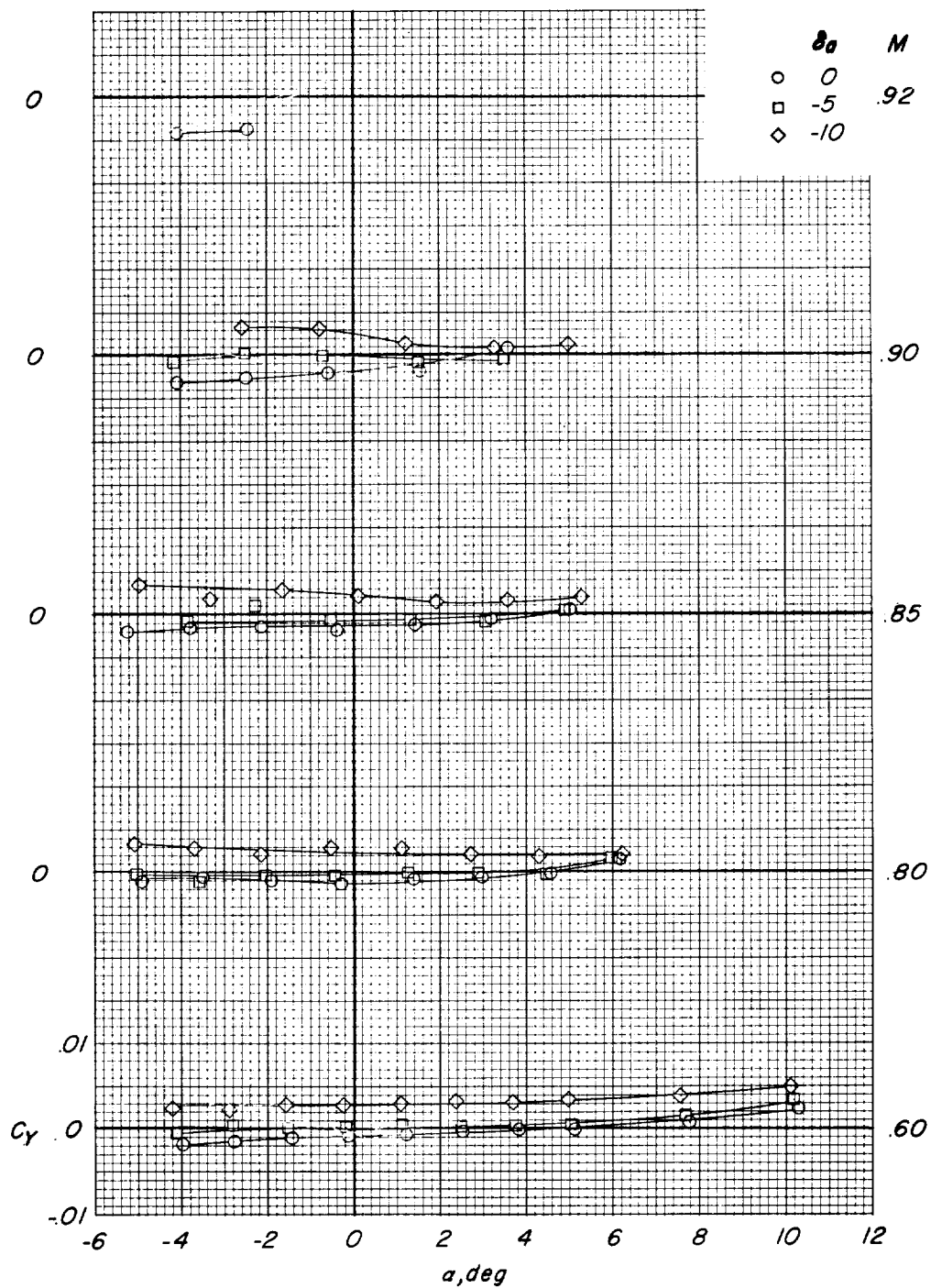
(a) Rolling-moment coefficients.

Figure 10.- Effectiveness of conventional aileron.



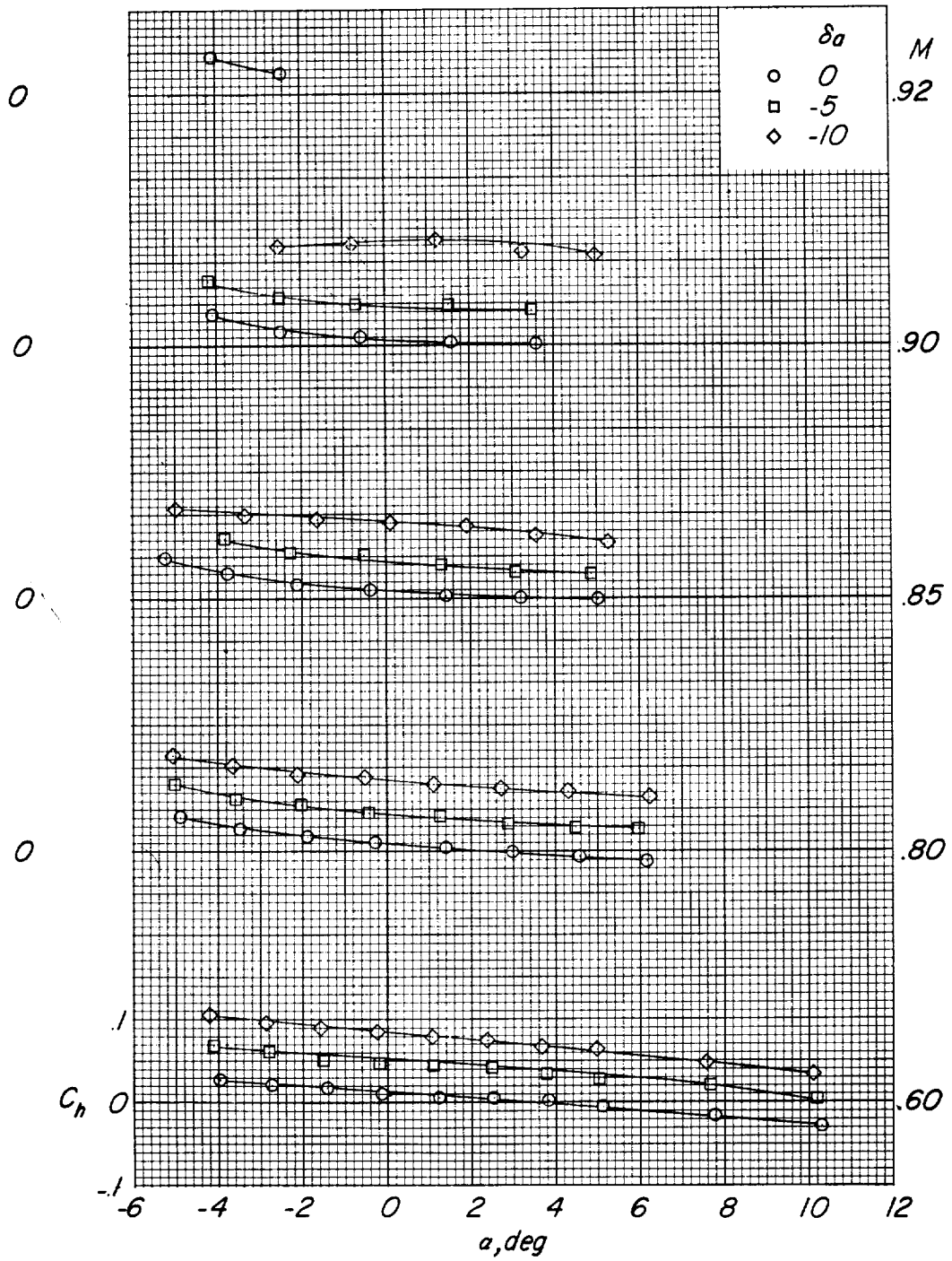
(b) Yawing-moment coefficients.

Figure 10.- Continued.



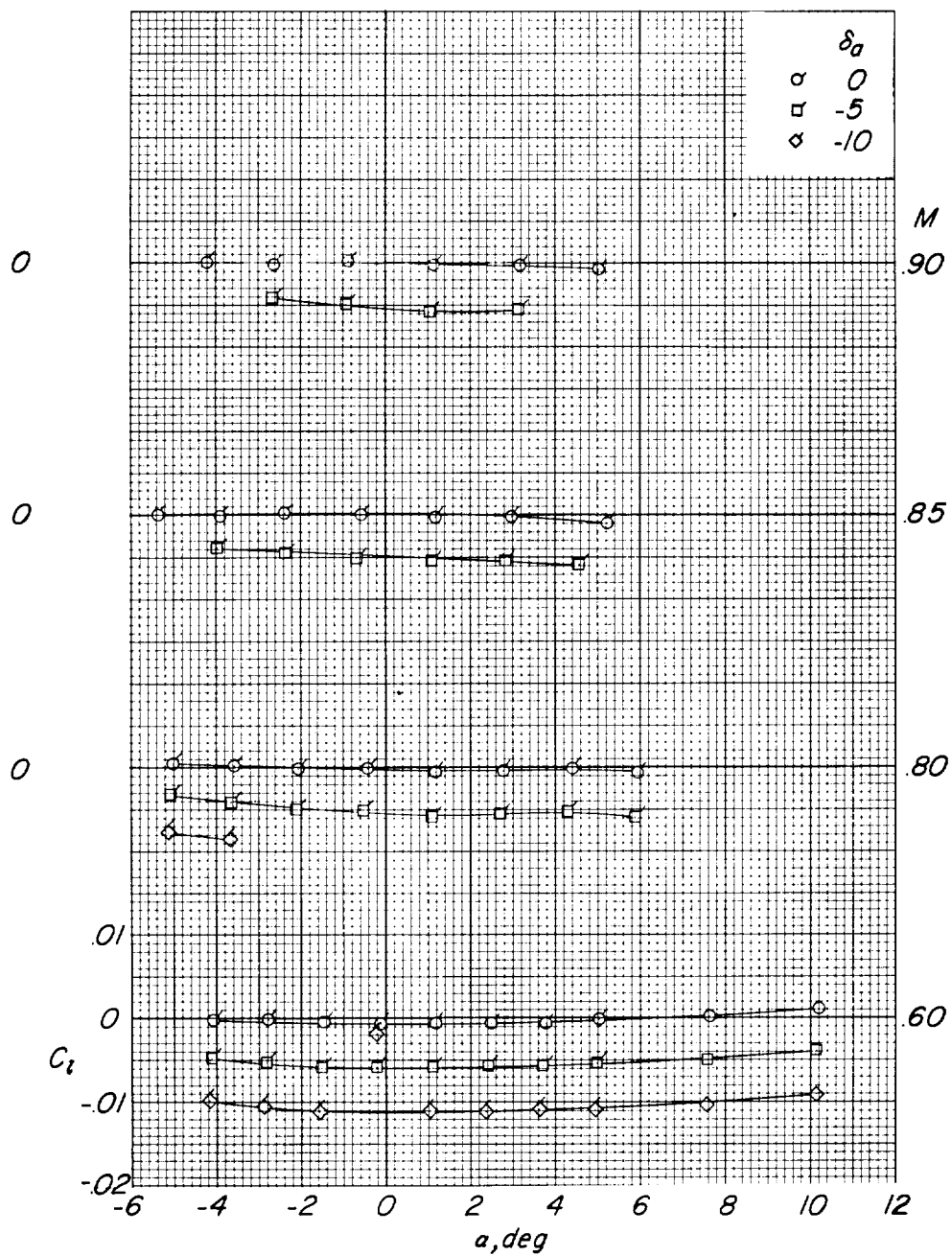
(c) Side-force coefficients.

Figure 10.- Continued.



(d) Hinge-moment coefficients.

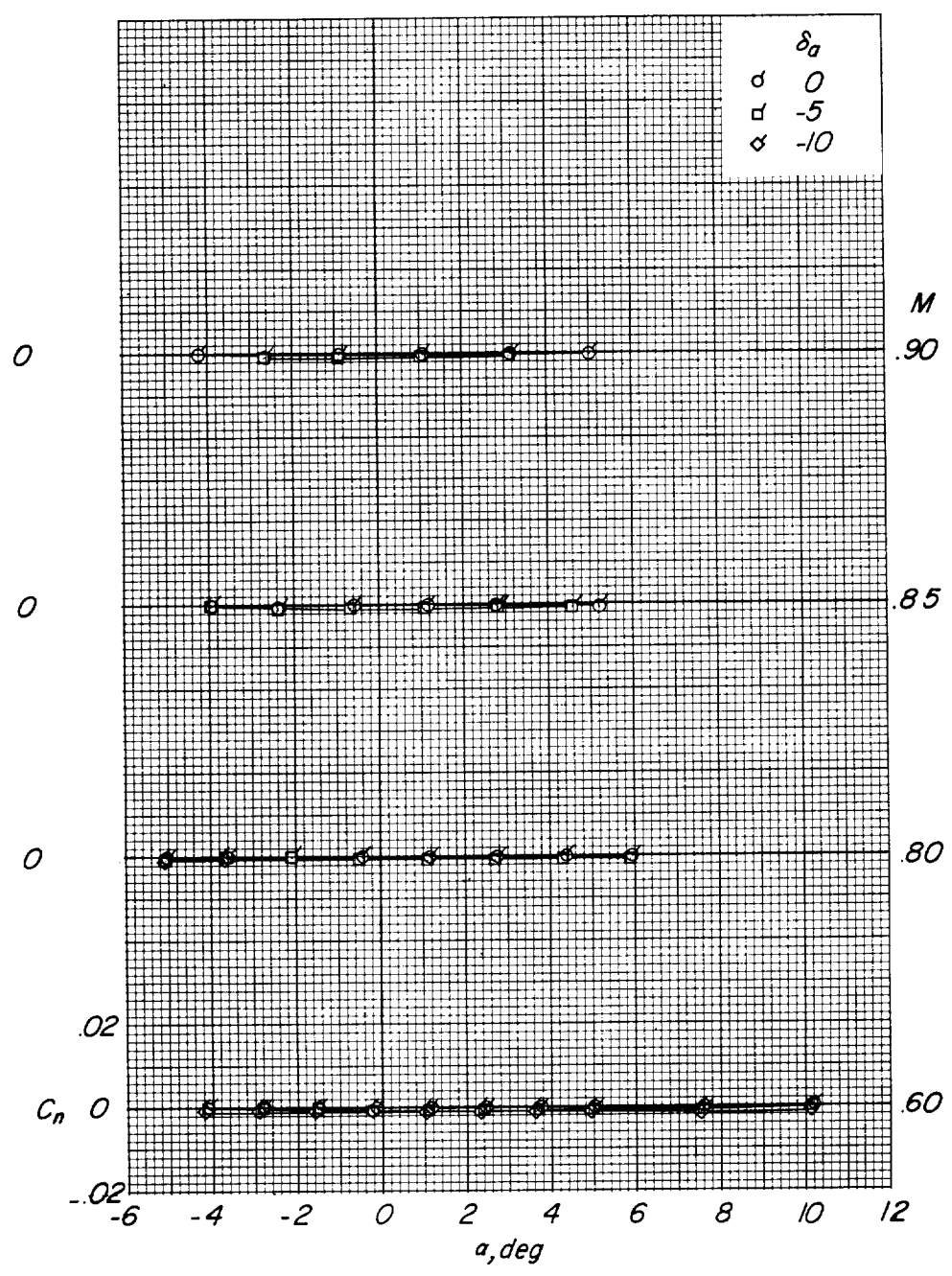
Figure 10.- Concluded.



(a) Rolling-moment coefficients.

Figure 11.- Aileron effectiveness in the presence of the inboard spoiler projected $0.05\bar{c}$.

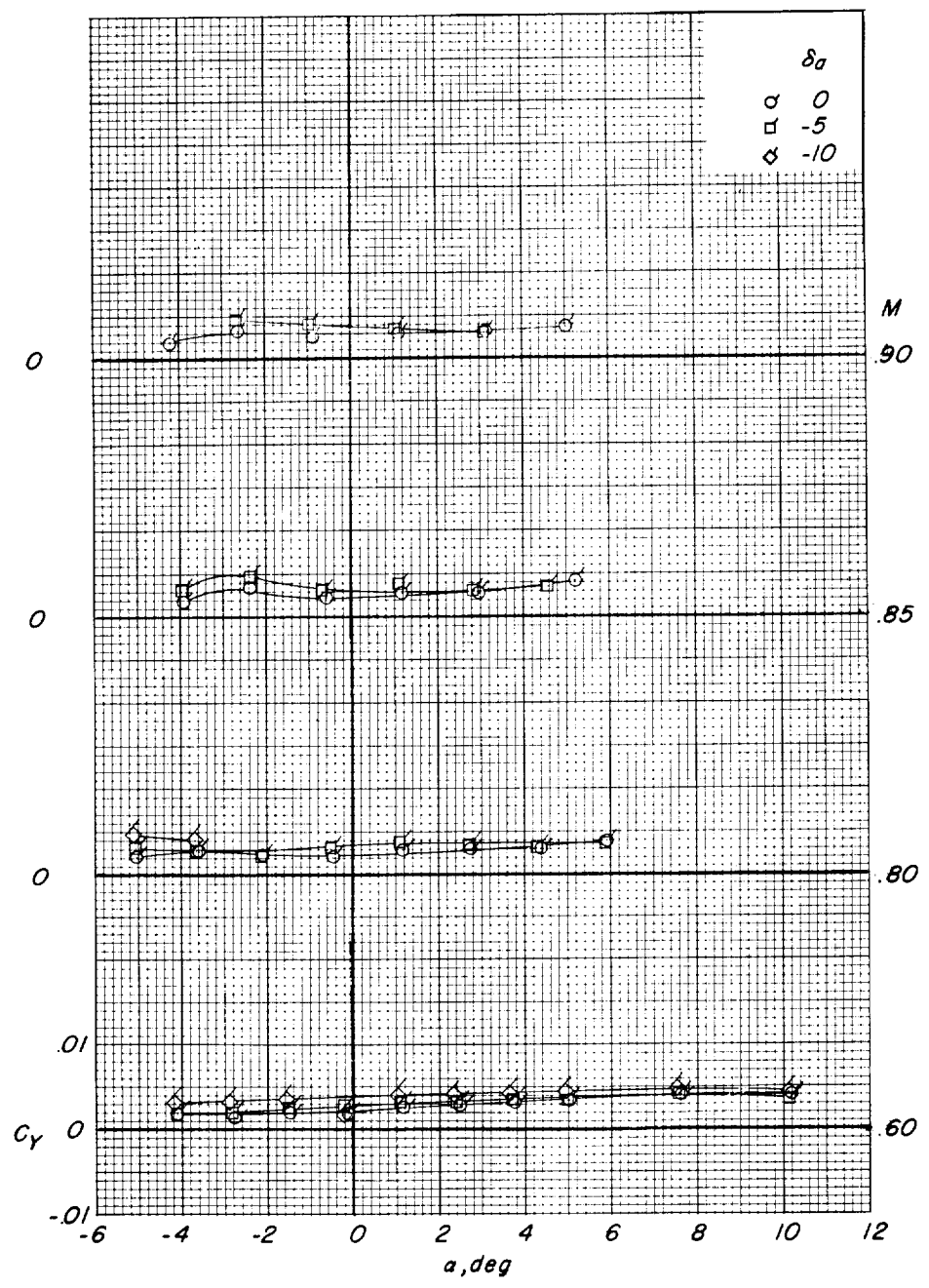
XXXXXXXXXX



(b) Yawing-moment coefficients.

Figure 11.- Continued.

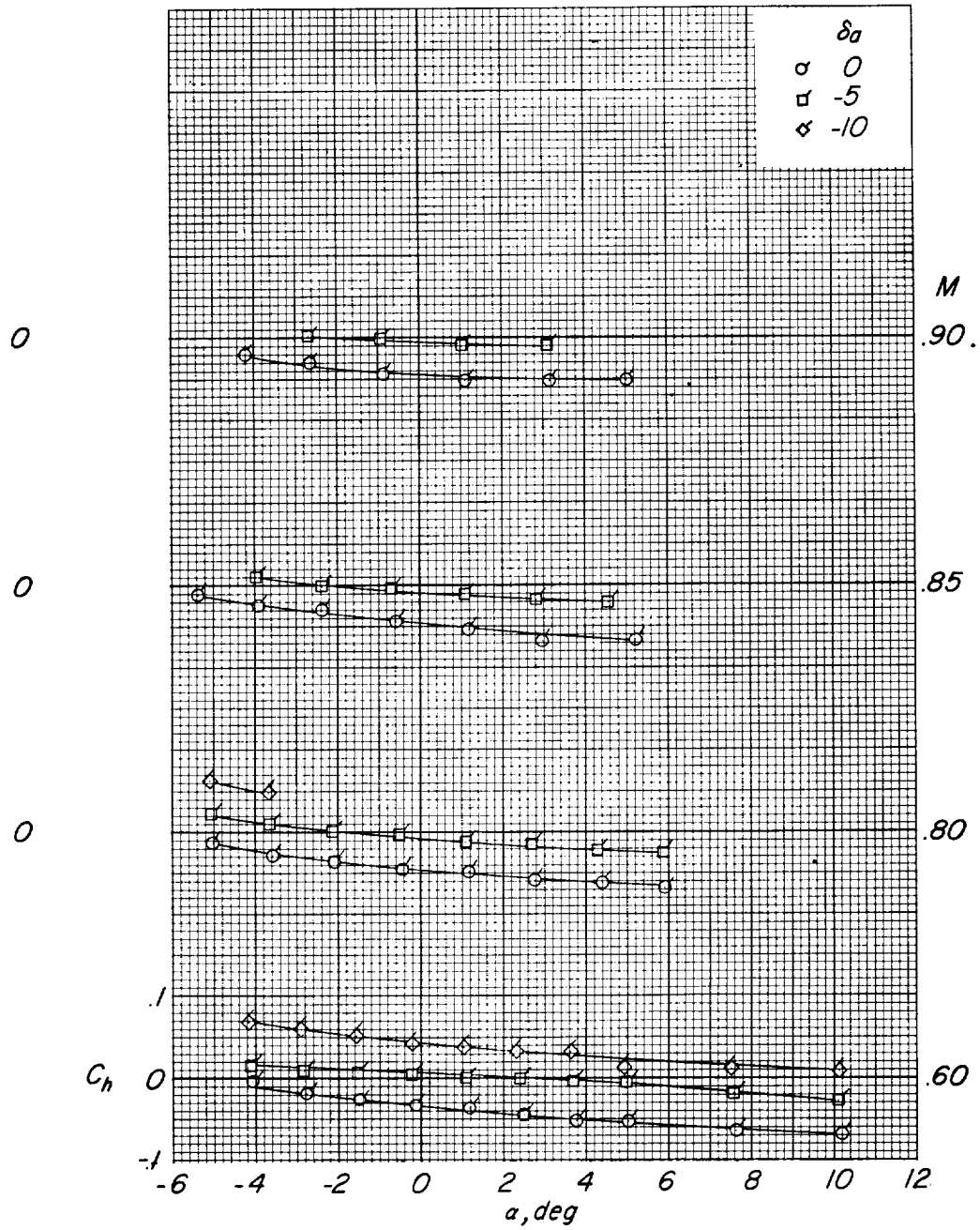
XXXXXXXXXX



(c) Side-force coefficients.

Figure 11.- Continued.

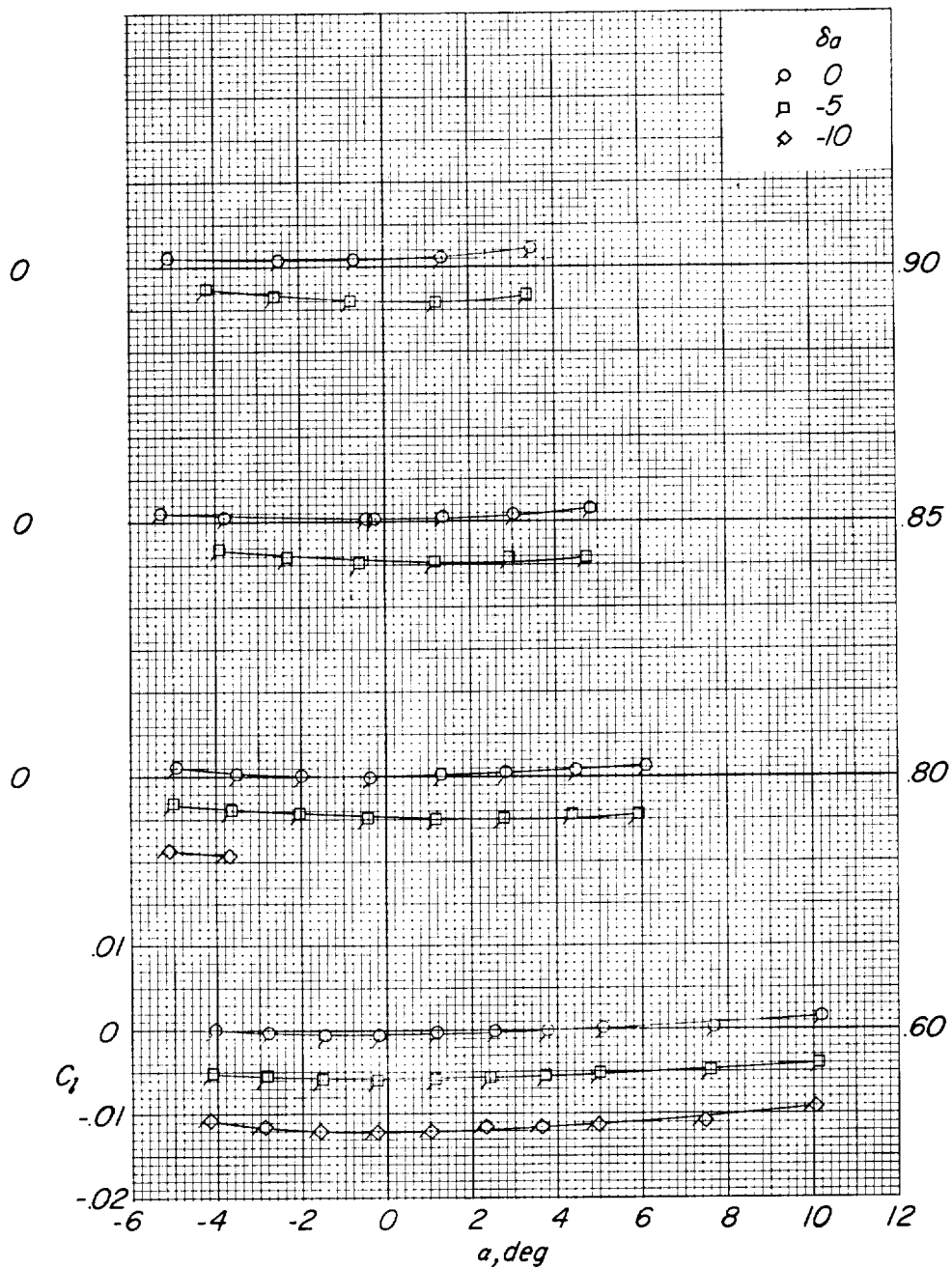
CONFIDENTIAL



(d) Hinge-moment coefficients.

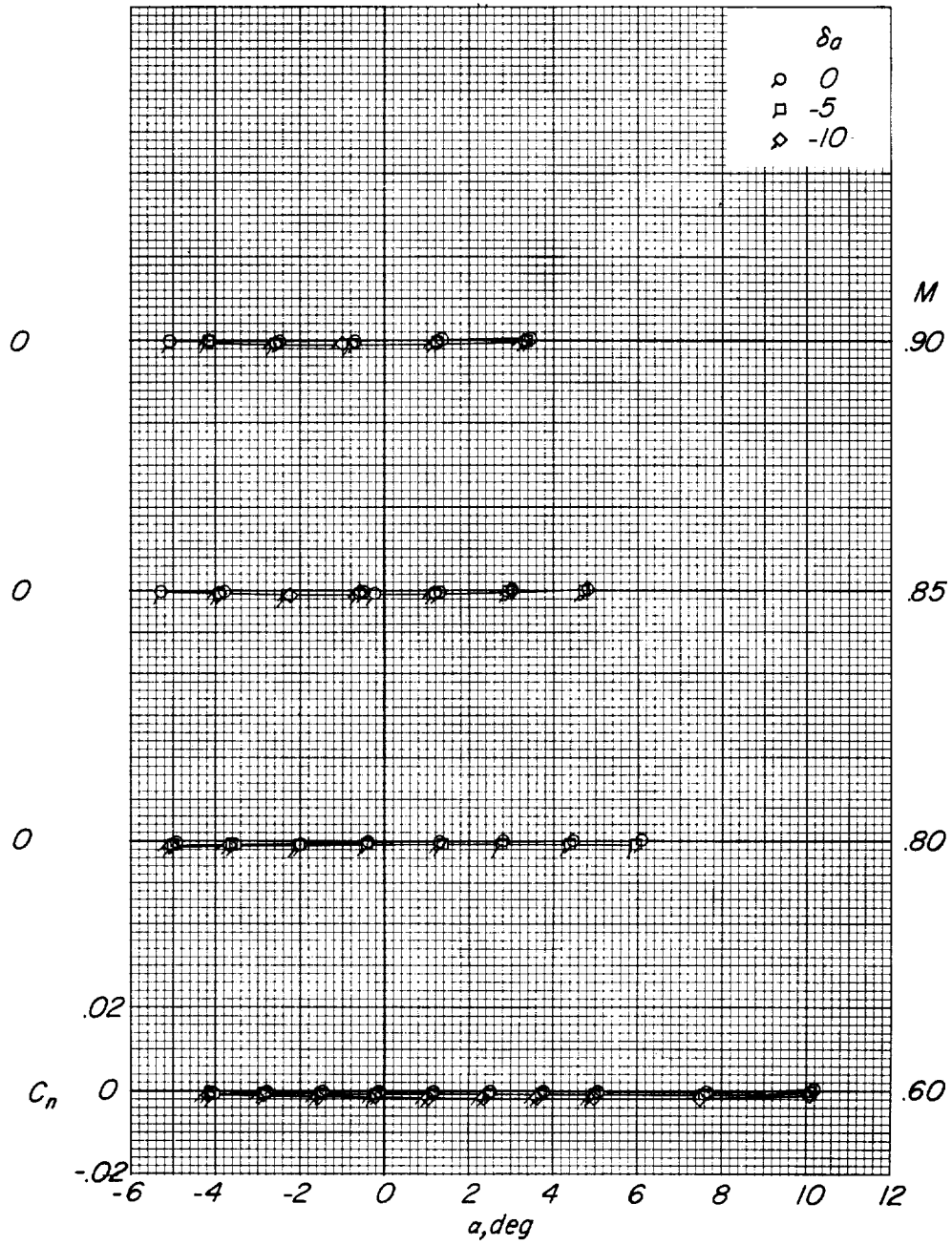
Figure 11.- Concluded.

CONFIDENTIAL



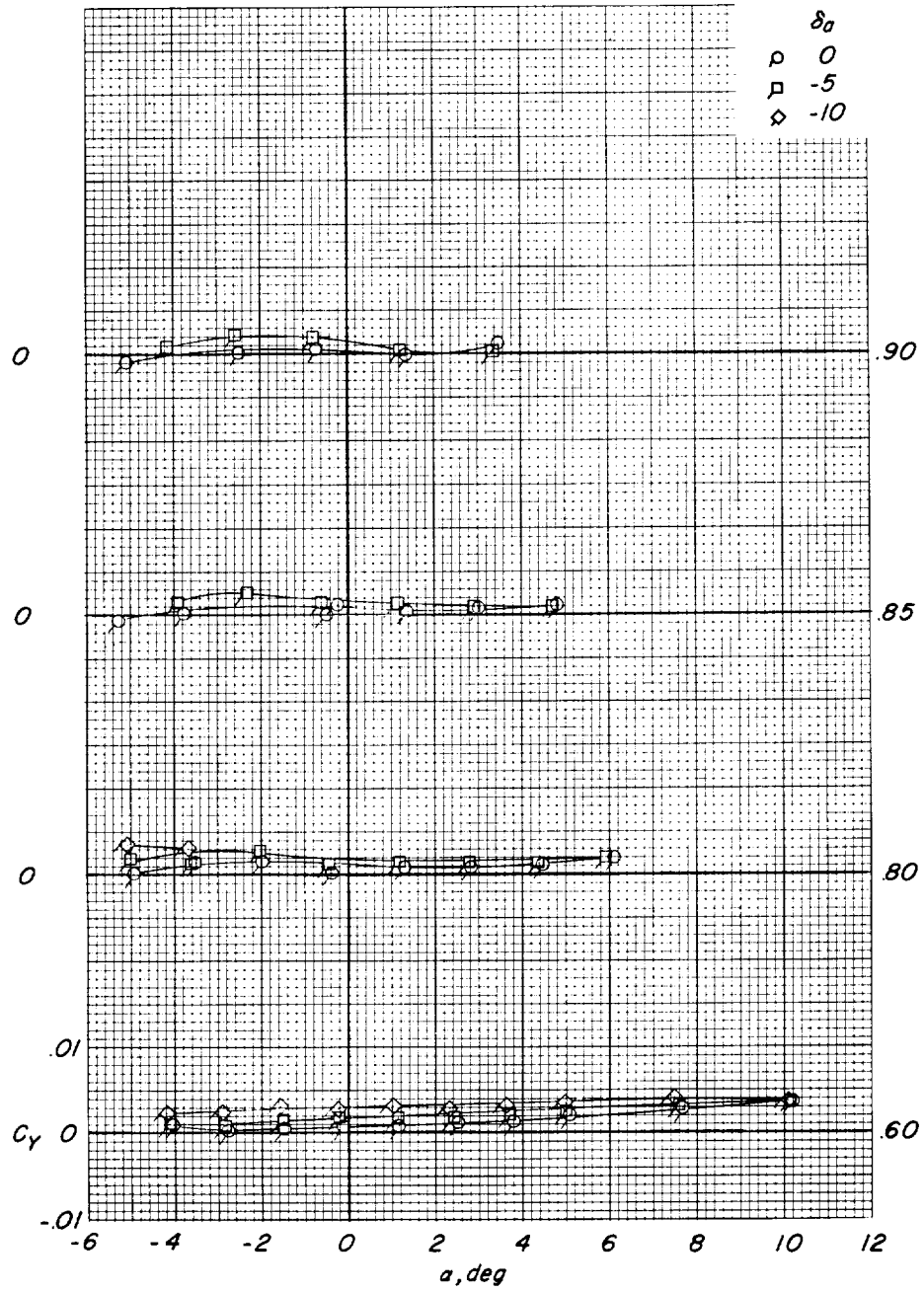
(a) Rolling-moment coefficients.

Figure 12.- Aileron effectiveness in the presence of the outboard spoiler projected $0.05\bar{c}$.



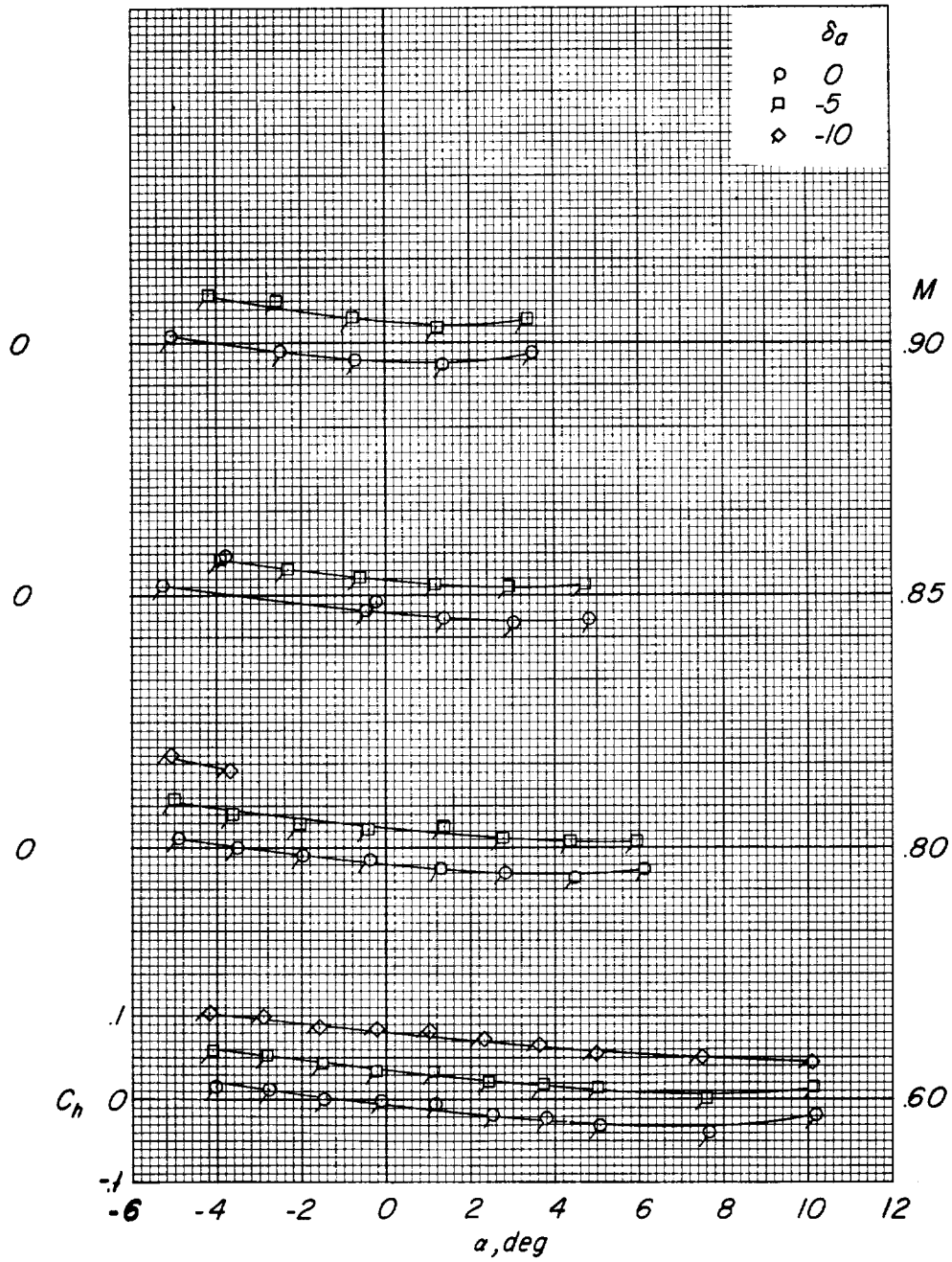
(b) Yawing-moment coefficients.

Figure 12.- Continued.



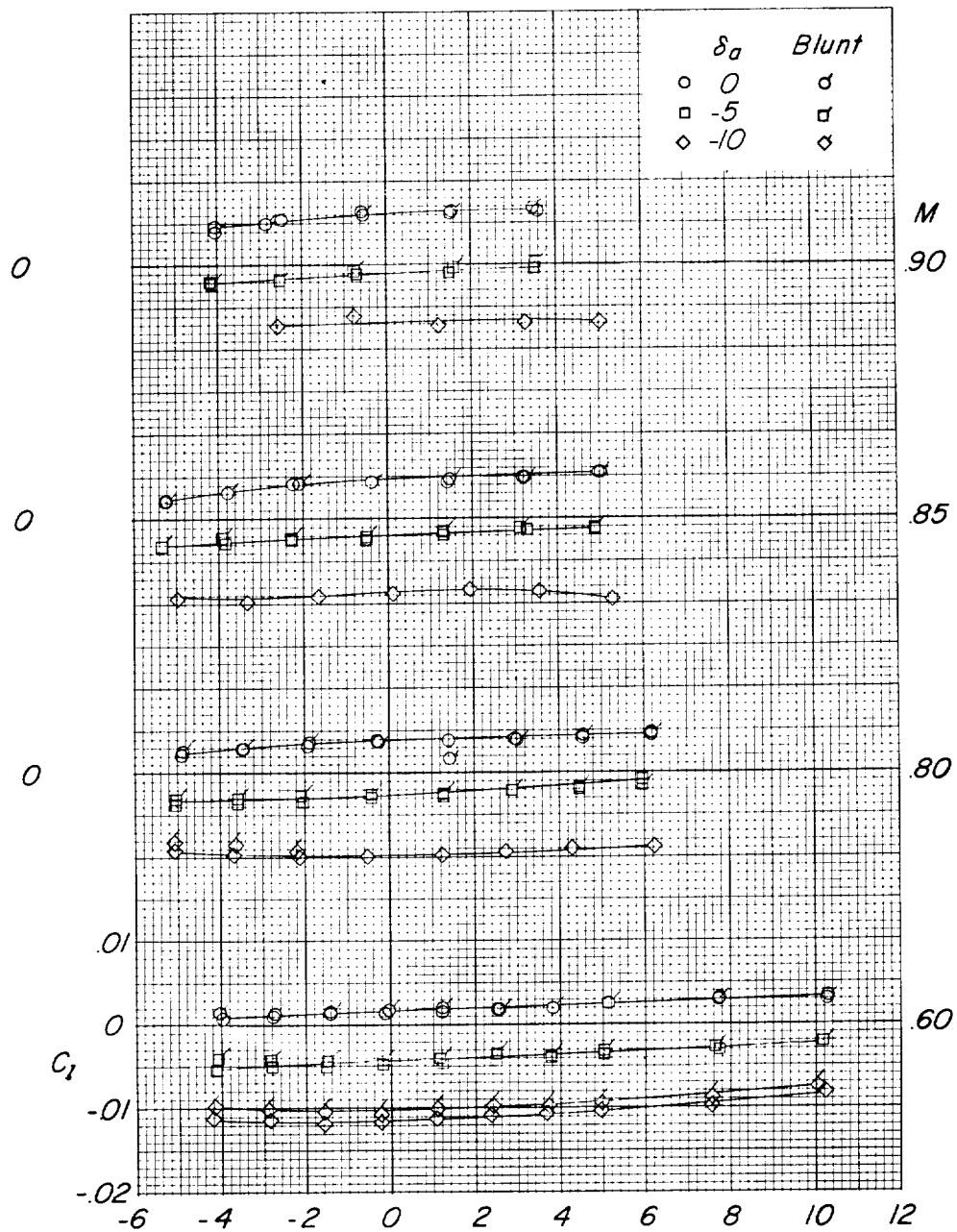
(c) Side-force coefficients.

Figure 12.- Continued.



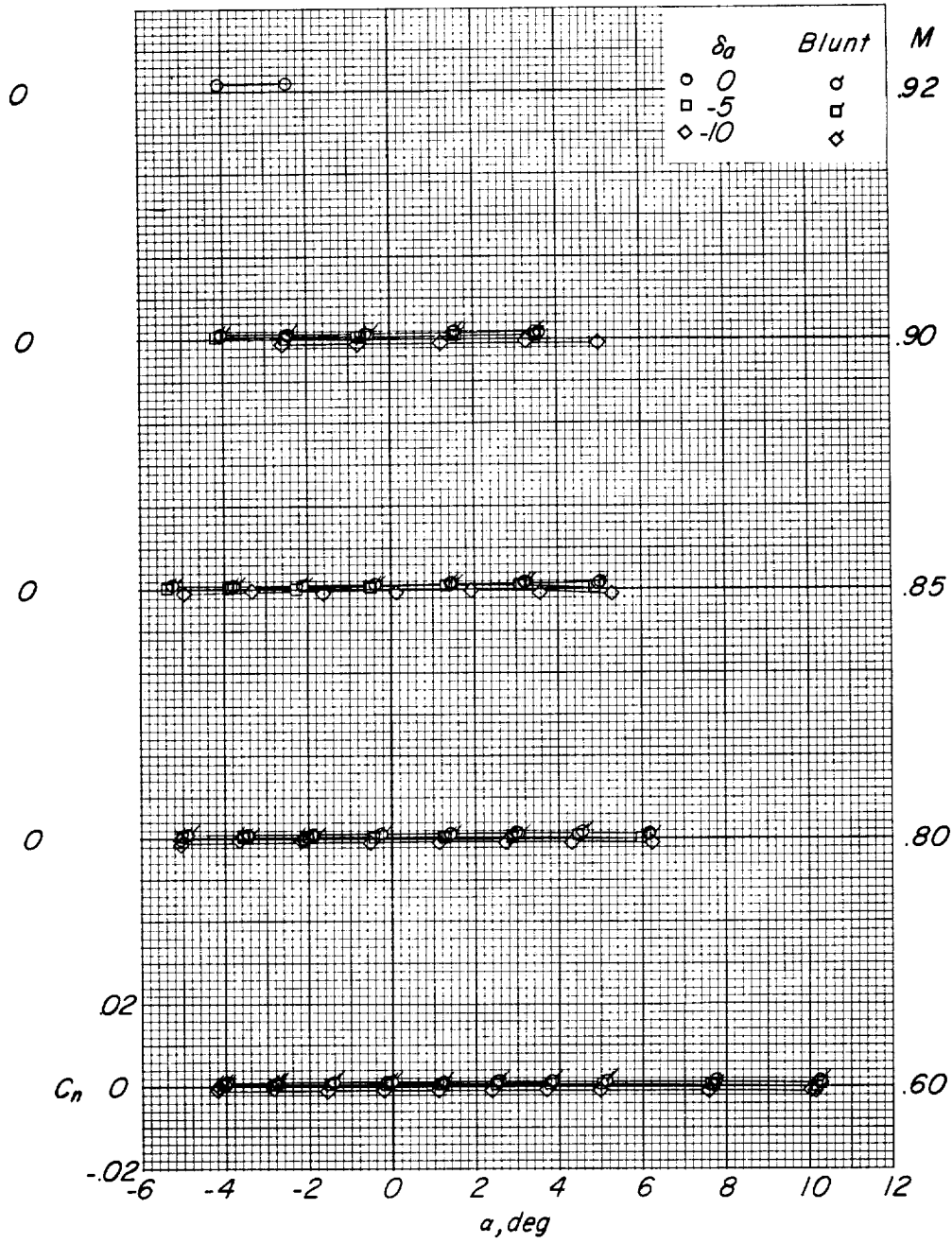
(d) Hinge-moment coefficients.

Figure 12.- Concluded.



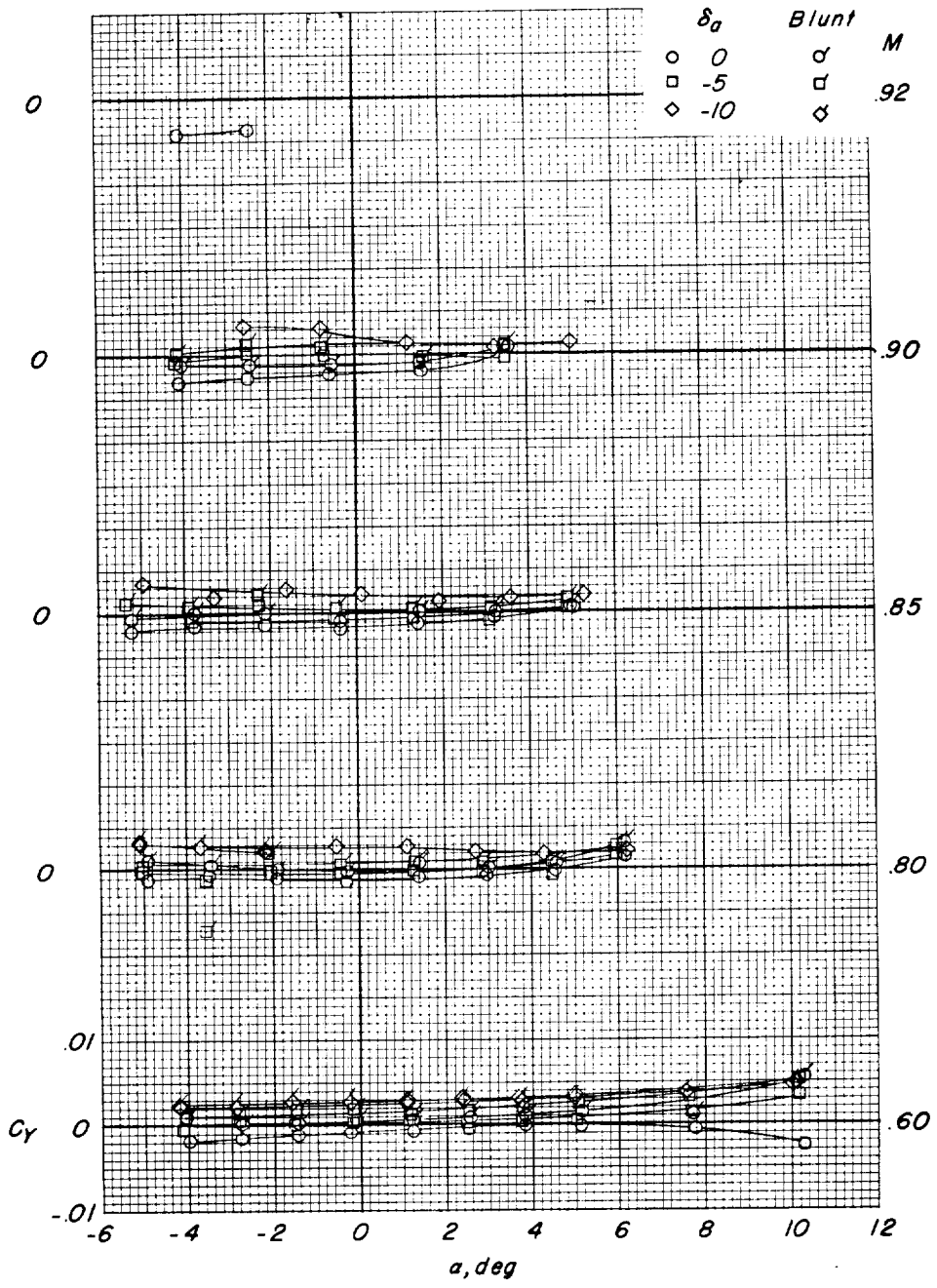
(a) Rolling-moment coefficients.

Figure 13.- Comparison of conventional and blunt trailing-edge aileron effectiveness.



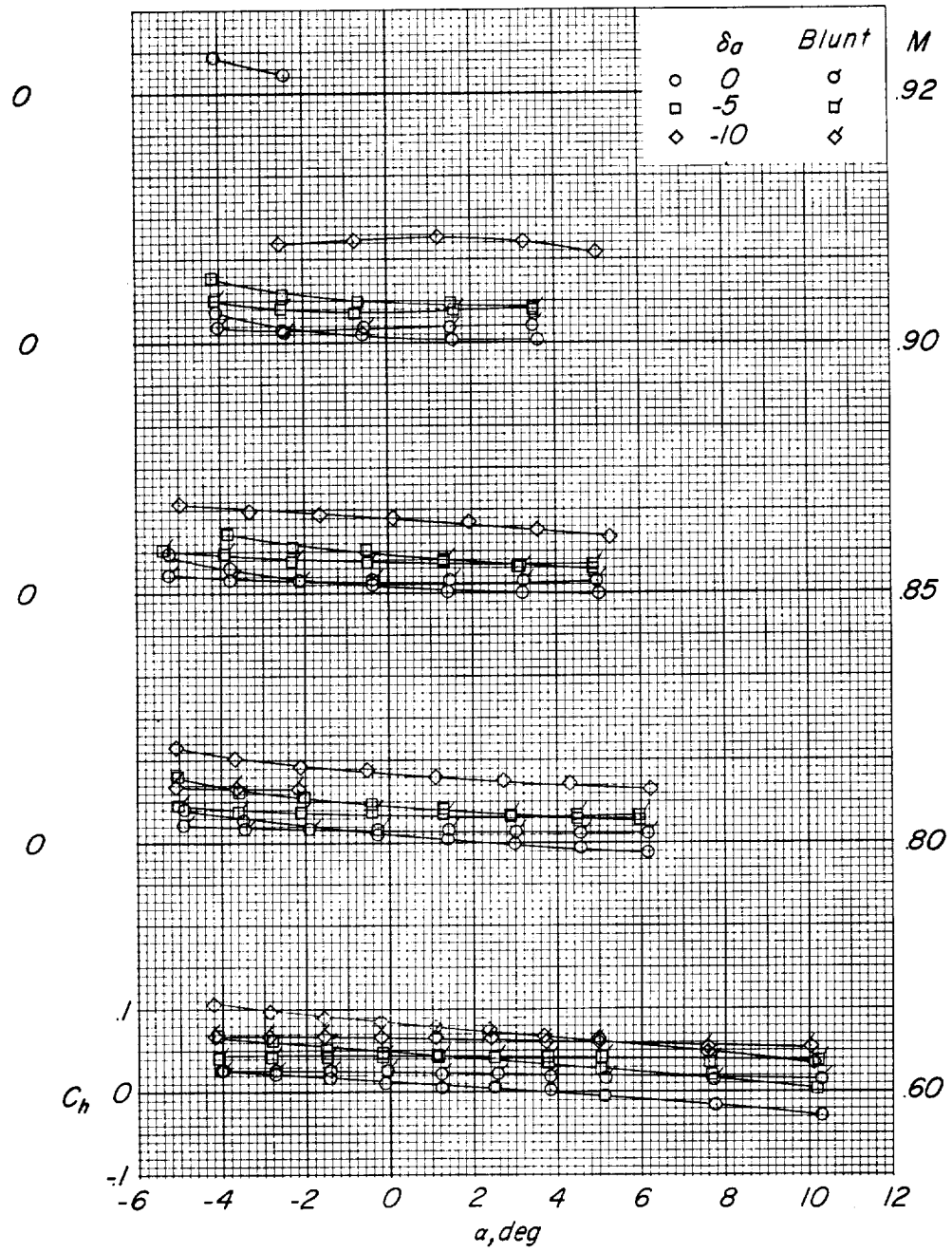
(b) Yawing-moment coefficients.

Figure 13.- Continued.



(c) Side-force coefficients.

Figure 13.- Continued.



(d) Hinge-moment coefficients.

Figure 13.- Concluded.

Longitudinal station

32.71 ———
 33.81 - - - -
 34.71 ———
 35.71 - - - -

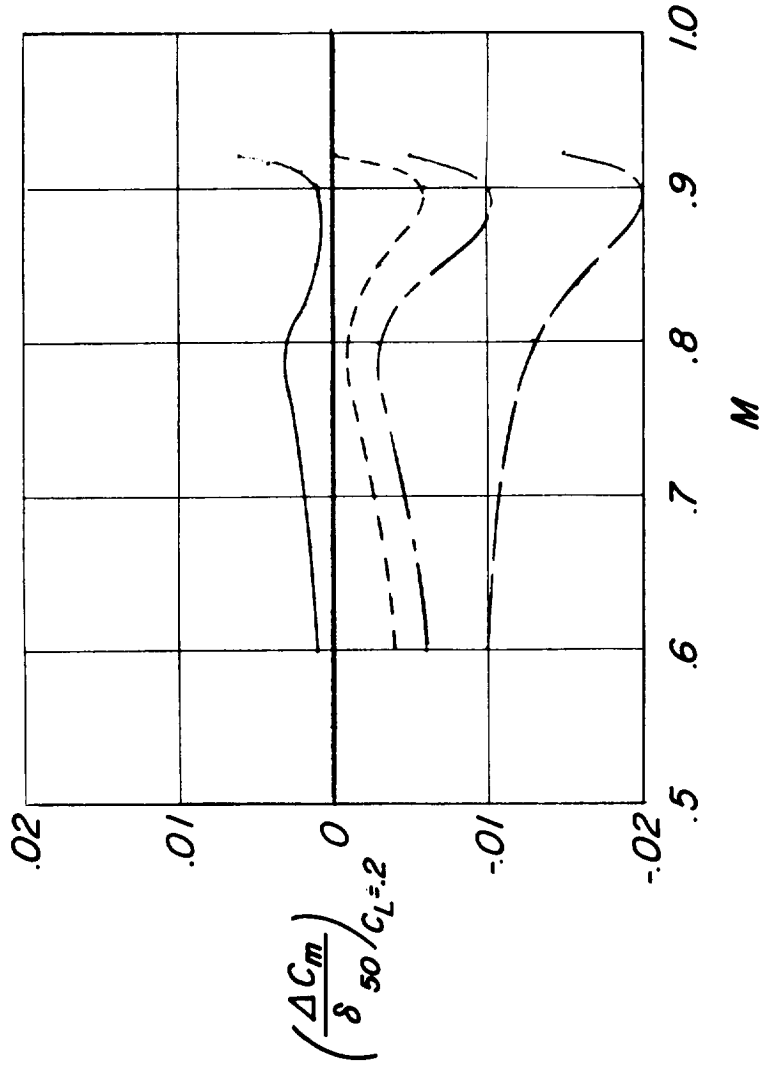


Figure 14.- Summary of pitch increments due to deflecting both underfuselage and side speed brakes 50° . $C_L = 0.2$; $\delta_a = 0.4$ inch.

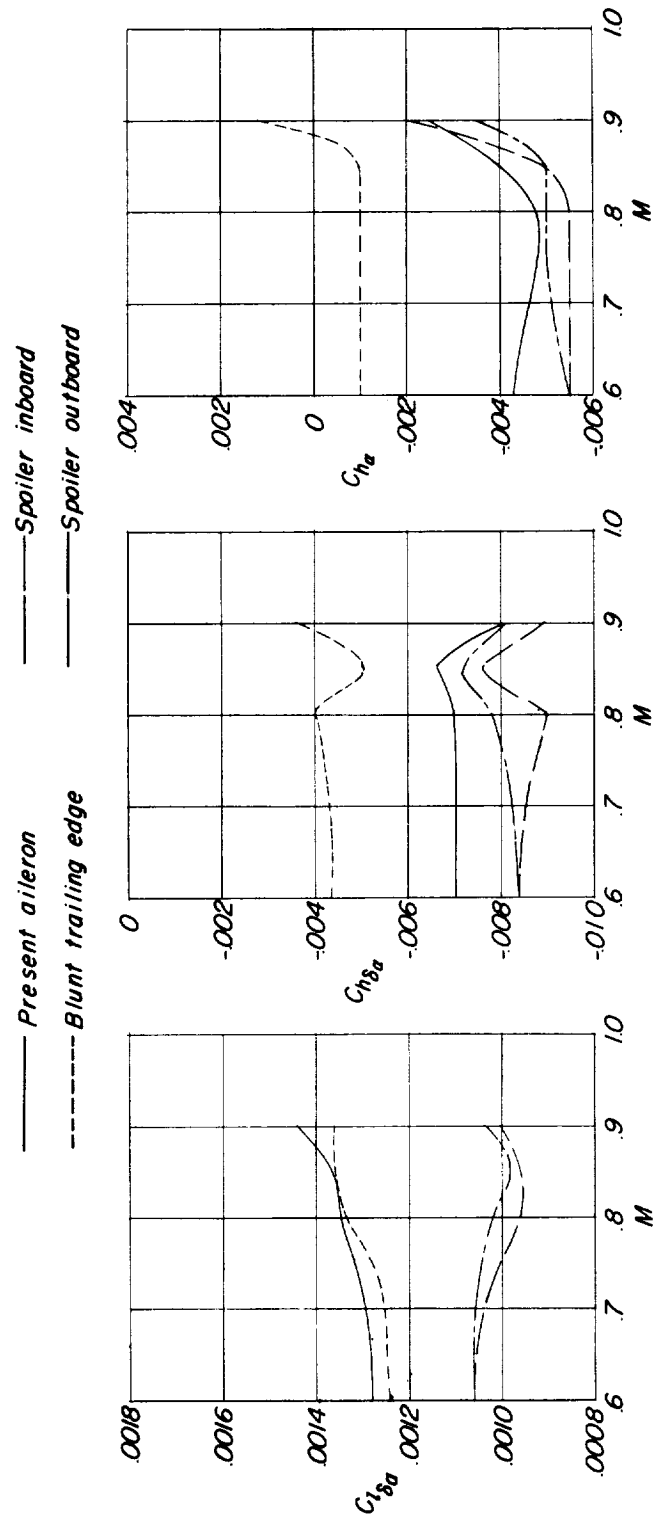


Figure 15.- Summary of aileron effectiveness including the effect of blunting the aileron trailing edge and of installing spoilers projected 0.05c ahead of the aileron at two spanwise locations.